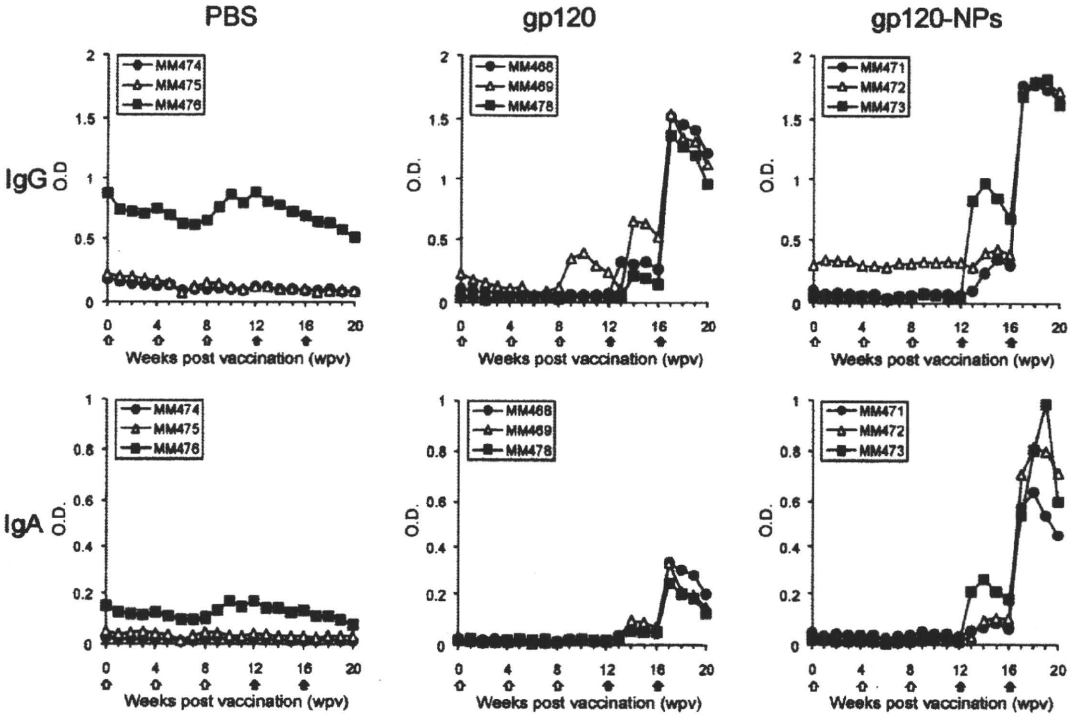

Fig. 2. Anti-HIV-1 gp120 IgG and IgA antibody levels in the plasma of macaques immunized with gp120-NPs, gp120-alone and PBS control. Plasma samples were collected at an interval of 1-week. The levels of gp120-specific IgG and IgA antibodies were measured by ELISA. Plasma samples were assayed after 100-fold dilution. The data are expressed as the optical density (O.D.). The white arrows indicate the times of intranasal immunization, and the black arrows indicate the times of subcutaneous immunization.

were clearly increased. A higher titer was detected in all macaques from the gp120-NP group than in the gp120-alone group. Thus, additional subcutaneous immunizations of 300 μg of gp120 antigen induced clear immune responses in the macaques, although the first 3 bouts of intranasal immunizations with 100 μg of gp120 antigen were insufficient. The induced cellular and humoral immune responses were higher in the gp120-NP group than in the gp120-alone group.

3.2. Intravenous challenge of the vaccinated macaques with SHIV-KU-2

To evaluate the protective effects provided by immunization with gp120-NP, a pathogenic virus, SHIV-KU-2, was intravenously challenged to vaccinated macaques 4 weeks after the last immunization. The plasma viral RNA load and $CD4^+$ T cell counts in the peripheral blood were then monitored.

The plasma viral RNA load in two macaques from the PBS group (MM474 and 475) increased with a peak of 10^6–10^7 copies/ml at 1-week post challenge (wpc), and one macaque (MM476) showed over 10^8 copies/ml after 2 wpc. Then, the viral load in all macaques decreased to below the 10^4 copies/ml after 10 wpc (Fig. 3). On the other hand, in all macaques from the gp120-alone and gp120-NP groups, the viral RNA load peaked at over 10^8 copies/ml at 2 wpc. Furthermore, two of the three macaques in the gp120-NP group (MM472 and 473) showed over 10^6 copies/ml after 10 wpc, although the viral RNA load of the other macaques decreased to below 10^5 copies/ml at those time points. Thus, the challenged virus had replicated more in the vaccinated groups than in the PBS control group. Furthermore, this tendency was more intense in the gp120-NP group than in the gp120-alone group.

The number of $CD4^+$ T cells in the peripheral blood of all macaques in the gp120-alone and gp120-NP groups decreased drastically to below 20% of the pre-challenge levels by 3 wpc, although the $CD4^+$ T cells were not so severely decreased in two of the three macaques in the PBS control group (MM474 and 475) (Fig. 4A). Thereafter, in two macaques from the gp120-NP group (MM472 and MM473) and one macaque from the gp120-alone group (MM469) remained below 20% of the pre-challenge levels until 12 wpc, according to the results of the plasma viral RNA load. Thus, the $CD4^+$ T cells in the peripheral blood were more severely decreased in the vaccinated groups than in the PBS control group. Furthermore, this tendency was more pronounce in the gp120-NP group than in the gp120-alone group.

To understand the decrease in the $CD4^+$ T cell population in the peripheral blood in more detail, we analyzed the $CD4^+$ T cell subpopulations using a CD95 marker. In two of the three macaques from the PBS group (MM474 and MM475), the $CD95^-$ naive $CD4^+$ T cell subpopulation remained over 30% after challenge (Fig. 4B). On the other hand, in all macaques from the gp120-alone and gp120-NP groups and one macaque from the PBS group (MM476), the naive $CD4^+$ T cell subpopulation decreased to below 20%. In all macaques, the $CD95^+$ memory $CD4^+$ T cell subpopulation transiently increased at 1 wpc and thereafter, in most of the macaques, it was maintained at the pre-challenge levels (20–40%) except for two macaques from the gp120-NP group (MM472 and MM473). The memory $CD4^+$ T cell population of these macaques decreased to below 10% after 3 wpc, and did not recover until 12 wpc (data not shown). Thus, in those macaques who showed a high viral load and severe $CD4^+$ T cell depletion, the memory $CD4^+$ T cell subpopulation was more severely injured as compared to the other macaques.

3.3. Virus-specific immune responses after the challenge infection of SHIV-KU-2

To assess the systemic immune responses in vaccinated macaques after the intravenous challenge infection, the virus-specific antibody levels in the plasma of macaques challenged

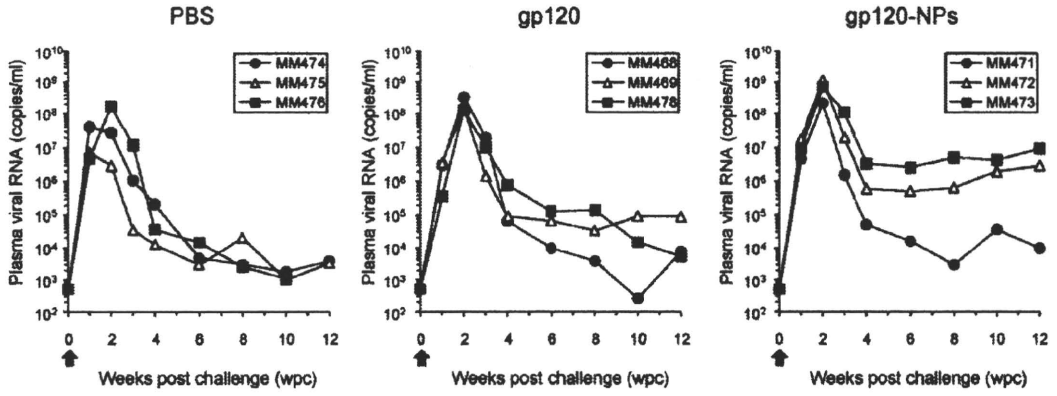

Fig. 3. Plasma viral RNA loads in the peripheral blood of SHIV-KU-2 infected macaques after intravenous inoculation with SHIV-KU-2. The unimmunized (PBS) and immunized (gp120-alone and gp120-NPs) macaques were intravenously challenged with SHIV-KU-2. The plasma viral RNA loads were measured by RT-PCR with a detection limit of 5×10^2 copies/ml. The black arrows indicate the time of challenge with SHIV-KU-2.

with SHIV-KU-2 were measured by the particle agglutination test (Table 1). In the gp120-alone and gp120-NP groups, the initial antibody responses were delayed as compared to the PBS group. In particular, MM472 and MM473 of the gp120-NP group had high viral loads, and the antibody titers were also low in these macaques. These results suggest that there was no protective effect against SHIV-KU-2 in both gp120-NP and gp120-alone groups, in contrast to the immunization-increased viral proliferation.

To assess the effects of the immunization, the lymphocyte proliferation activities after SHIV-KU-2challenge were measured by determining the ratio of Brd-U incorporated by PBMCs in the presence of HIV-1 gp120 and SIV p27 (Fig. 5). First, the gp120-specific lymphocyte proliferation activities were increased in two macaques from the PBS group at 2, 4 (MM476) and 8 wpc (MM475). In two macaques from the gp120-alone group (MM468 and MM469), an increase in proliferative activities could be detected at 2 and 3 wpc. On the other hand, in three macaques from the gp120-NP group, an increase in proliferative responses was observed after 1 wpc (MM472 and MM473) and 2 wpc (MM471). In other words, the increase in activity in the gp120-NP group could be detected earlier than any other group. p27-specific lymphocyte proliferation activities were increased in three macaques from the PBS group at 2 wpc (MM475 and MM476) and 3 wpc (MM474). After 4 wpc in the PBS group, higher proliferative responses were observed in

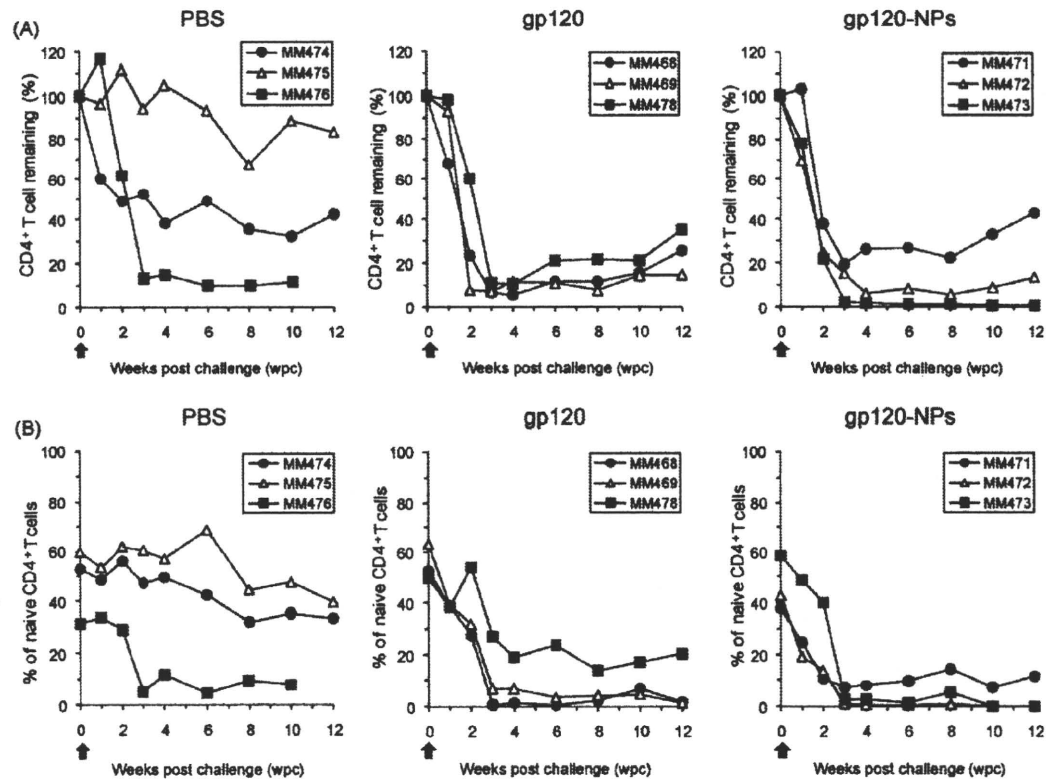

Fig. 4. The number of (A) $CD4^+$ T cells and (B) $CD95^-$ naive $CD4^+$ T cells in the peripheral blood of SHIV-KU-2 infected macaques after an intravenous inoculation with SHIV-KU-2. (A) The number of $CD4^+$ T cells was determined by flow cytometry. The data are expressed as a percent of the cell counts immediately before challenge. (B) Sequential changes in the proportion of the subpopulation (CD95 negative naive cells) of the peripheral blood $CD4^+$ T cells. The percentage of these cells in the $CD4^+$ T cells was determined by flow cytometry. The black arrows indicate the time of challenge with SHIV-KU-2.

Table 1
HIV-1/2 specific antibody responses in the plasma obtained from vaccinated macaques after the intravenous SHIV-KU-2 challenge.

Groups	Macaques	Weeks post challenge (wpc)							
		1	2	3	4	6	8	10	12
PBS	MM474	n.d.	4096	>16,384	>16,384	>16,384	>16,384	>16,384	>16,384
	MM475	n.d.	4096	>16,384	>16,384	>16,384	>16,384	>16,384	>16,384
	MM476	n.d.	8192	>16,384	>16,384	>16,384	>16,384	>16,384	-
gp120	MM468	n.d.	1024	1024	4096	>16,384	>16,384	>16,384	>16,384
	MM469	n.d.	4096	>16,384	>16,384	>16,384	>16,384	>16,384	>16,384
	MM478	n.d.	256	512	8192	>16,384	>16,384	>16,384	>16,384
gp120-NPs	MM471	n.d.	4096	>16,384	>16,384	>16,384	>16,384	>16,384	>16,384
	MM472	32	4096	4096	2048	>16,384	8192	4096	2048
	MM473	n.d.	1024	1024	256	512	512	256	128

Antibodies to HIV *gag* p24 and *env* gp41 in the plasma were measured by the PA method. The data indicated as the titer of serial dilution. n.d.: not detected.

all macaques. In all macaques from the gp120-alone group, the increase in activity could be detected after 2 wpc. On the other hand, in only one macaque from the gp120-NP group (MM471) with a low viral load, an increase in activity was observed after 3 wpc. In the gp120-NP and gp120-alone groups, an increased plasma viral RNA load, and a reduction in $CD4^+$ T cells in the peripheral blood, and gp120-specific lymphocyte proliferation were identified at 1–3 wpc. However, in the PBS group, p27-specific lymphocyte proliferation was identified at the same time, and was higher than in the immunized group after 4 wpc. These results suggest that immunization with gp120-NPs or gp120-alone enhanced gp120-specific immunity, but immunity to the gp120 antigen did not become effective against viral infection or viral proliferation.

4. Discussion

Polymeric nanoparticles have been investigated as an efficient delivery system to APCs for a protein antigen [40]. Therefore biodegradable NPs consisting of γ-PGA derived from *Bacillus* represent a system with efficient immune induction [41–48] and safety [45,46], since it is specifically taken up by dedicated APCs such as DCs [34,44], and is easily disintegrated by proteases [49]. In immune induction experiments using mice with HIV-1 *env*-gp120 carrying γ-hPGA NPs (gp120-NPs), it was shown that both cellular and humoral immune responses were efficiently induced by a low number of vaccinations, suggesting the possibility of use as an efficient vaccine candidate for HIV-1 infection [36]. However, it is unknown whether the immune responses induced in the mouse have protective effects against HIV infection, because HIV-1 is not contagious to mice. Therefore, we immunized rhesus macaques with gp120-NPs in this study to clarify the immune induction capabilities of gp120-NPs and their protective effects against viral infection using a SHIV infection system, because this could not be confirmed with the mouse model.

In the mouse experiments, potent specific cellular immunity was induced with a single intranasal administration of gp120-NPs

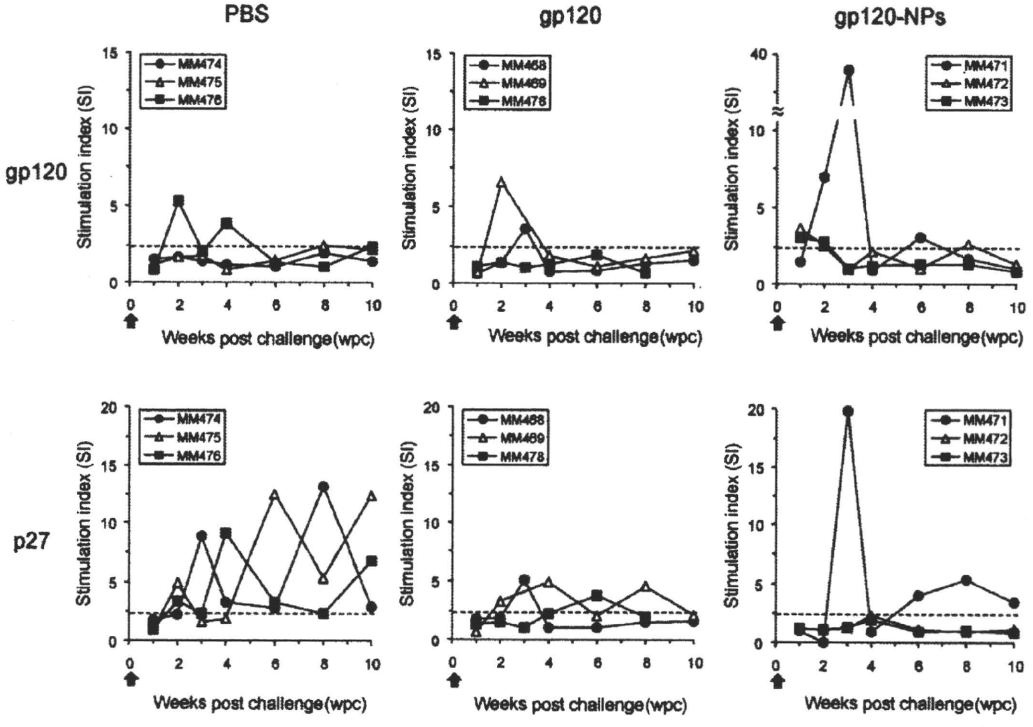

Fig. 5. Antigen-specific lymphocyte proliferation responses in PBMCs from macaques challenged with SHIV-KU-2. The proliferation of the PBMCs was measured by Brd-U uptake after stimulation with gp120 or p27, and was expressed as a stimulation index (SI) as described in Section 2. The cut off value is 2.5 for the SI. The arrows indicate the time of challenge with SHIV-KU-2.

[36]. It has also been reported that mucosal immunization with an HIV-1 vaccine can induce mucosal and systemic HIV-1-specific humoral and cellular immune responses in macaques [20,50,51]. Therefore, we selected intranasal immunization as the administration route of vaccines. However, we determined that three intranasal administrations with 100 μg of gp120-NPs were not able to induce a sufficient immune response in the macaques. Therefore, we performed two additional subcutaneous administrations with 300 μg of gp120-NPs. In this experiment, 100 μg of gp120 was used for each nasal administration. This quantity was decided by a calculation from the optimal amount per weight obtained from mouse experiments. Other research groups administered it intramuscularly or subcutaneously, with more amount of gp120, and obtained antigen-specific cellular immunity and antibody responses [52,53], although they used a different antigen delivery system. In our particulate delivery system, a greater amount of antigen was necessary to induce a specific immune response in macaques than in mice. An additional two subcutaneous administrations with 300 μg of gp120-NPs induced not only cellular immune responses, but also humoral antibody responses (IgG and IgA), which was poorly induced in the mouse experiments [35], indicating a boost effect in macaques. After the subcutaneous immunization, the increase in gp120-specific IFN-γ producing cells, the increase in gp120-specific cell proliferation activity and the anti-gp120 antibody titer (IgG and IgA) in the plasma were confirmed in all macaques immunized with gp120-NPs and gp120-alone. In both cellular and humoral immune responses, the degree of immune induction was clearly stronger in the gp120-NP immunized macaques than in the gp120-alone immunized macaques. Thus, it became clear that γ-hPGA NPs had an immune reinforcement effect not only in the mice, but also in the rhesus macaques. However, the numbers of gp120-specific SFCs in the gp120-NP group obtained from ELISPT assay were low at less than 10 spots per million PBMCs. These results suggest that antigen-specific CD8 T cell responses were not or poorly induced by the vaccination of gp120-NPs. Consequently, CD4 T cell responses were primarily enhanced in macaques immunized with gp120-NPs.

To examine the protective effects of the gp120-specific immune responses induced by gp120-NPs against viral infection, a challenge inoculation with pathogenic SHIV-KU2 was performed in immunized macaques. Against our expectations, no protective effect was observed. Instead, a promotion of viral growth was observed in immunized macaques as compared to naive control macaques. Furthermore, the degree of reinforcement of the infection was stronger in the gp120-NP immunized macaques than in the gp120-alone immunized macaques. The gp120-specific immune responses induced by vaccination correlated with the promotion of viral growth in between groups. However, there was no definite the correlation between the immune responses and viral road of within-group. Since the target cells for primate lentivirus infection are immune cells such as $CD4^+$ T cells and macrophages, the only useful immune reaction should be activated protection against viral infection. In other words, there is a case for promoting viral replication by inappropriate or insufficient immune responses. For example, there were some antibodies reinforcing the HIV-1 infection [54,55], and HIV-1 is preferentially contagious to memory $CD4^+$ T cells, which are specific for HIV-1 antigens [56]. In this study, we used gp120 as the antigen based on the result that the immune response against *env* was better than that against *gag* in a mouse study [36,37]. The number of $CD4^+$ T cells in the peripheral blood decreased conspicuously at the same time as the immune response specific for gp120 appeared early after virus inoculation in the gp120-NP and gp120-alone vaccinated groups. On the other hand, in the naive control group, the immune response specific for p27 (*gag*) was detected, but not the immune response specific for gp120 (*env*) early after the virus inoculation. Thus, the $CD4^+$ T cells in the peripheral blood were maintained without any decrease in 2 out of 3 naive control macaques. Recently, it has been reported that the strength of the specific immune response against *gag*, i.e. the internal protein structure of the virus is correlated to the decrease in the quantity of virus in the peripheral blood of HIV-1 infected patients. In contrast, the strength of the specific immune responses against the *env* in the crust protein and accessory proteins are correlated to the increase in the quantity of blood virus [57]. Our result that the vaccination of rhesus macaques inducing a specific immune response against *env*-gp120 showed an enhancement of viral replication was consistent with the observations in HIV-1 infected patients, supporting the importance of antigen selection for HIV-1 vaccine development. Moreover, some groups have recently argued that activated $CD4^+$ T cells induced by vaccination in macaques can be an attractive target for SIV infection [58,59]. It is likely that the macaques immunized with gp120-NPs were primarily enhanced gp120-specific CD4 T cell responses but not CD8 T cell. The balance of CD4 and CD8 T cell mediated responses induced by vaccination may be critical in determining viral exclusion and replication.

The total picture of the immune system which is truly important for infection control in individuals infected with the AIDS virus is not yet clarified, and the further accumulation of basic information about the immune correlates for protective immunity is necessary. In our previous project, the partial protective effects of viral replication was obtained in vaccinated macaques by using different nanoparticles connecting the inactivated whole virus particles, not a refined protein [28]. The whole virion is considered to include many kinds of antigens acting for infection restraint and/or promotion. It may be possible to induce only effective immune responses acting for infection restraint with a biodegradable nanoparticle vaccine, distinguishing the restraint-related and promotion-related antigens by a detailed examination of the antigen enclosed in the γ-hPGA NPs in the future. Although cell-mediated immunity against peptide epitopes of viral structural proteins is the mainstream for vaccine development research, other poorly analyzed target antigens such as glycolipids, lipoproteins and nuclear antigens may also have to be examined.

In this study, it was demonstrated that biodegradable nanoparticles composed of amphiphilic γ-PGA have a reinforcement effect for immune responses, and have an impact on important immune cell populations participating in viral replication in infected individuals, although the result was the opposite to our expectation. It is important to ascertain the correct antigen stimulation to guide the patient's immunity to act on infection defense and viral replication restraint effectively using a primate experimental infection model. These biodegradable nanoparticles are expected to be useful as an antigen delivery tool in AIDS vaccine development research.

Acknowledgment

This work was supported by CREST from the Japan Science and Technology Agency (JST).

References

[1] Letvin NL. Correlates of immune protection and the development of a human immunodeficiency virus vaccine. Immunity 2007;27:366–9.
[2] Pomerantz RJ, Horn DL. Twenty years of therapy for HIV-1 infection. Nat Med 2003;9:867–73.
[3] Chun TW, Fauci AS. Latent reservoirs of HIV: obstacles to the eradication of virus. Proc Natl Acad Sci USA 1999;96:10958–61.
[4] Zhao Z, Leong KW. Controlled delivery of antigens and adjuvants in vaccine development. J Pharm Sci 1996;85:1261–70.
[5] Singh M, O'Hagan D. Advances in vaccine adjuvants. Nat Biotechnol 1999;17:1075–81.
[6] Storni T, Kundig TM, Senti G, Johansen P. Immunity in response to particulate antigen-delivery systems. Adv Drug Deliv Rev 2005;57:333–55.
[7] Greenland JR, Letvin NL. Chemical adjuvants for plasmid DNA vaccines. Vaccine 2007;25:3731–41.

[8] O'Hagan DT, Lavelle E. Novel adjuvants and delivery systems for HIV vaccines. AIDS 2002;16:115–24.
[9] Reddy ST, Swartz MA, Hubbell JA. Targeting dendritic cells with biomaterials: developing the next generation of vaccines. Trends Immunol 2006;27:573–9.
[10] Waeckerle-Men Y, Groettrup M. PLGA microspheres for improved antigen delivery to dendritic cells as cellular vaccines. Adv Drug Deliv Rev 2005;57:475–82.
[11] Shibata R, Igarashi T, Haigwood N, Buckler-White A, Ogert R, Ross W, et al. Neutralizing antibody directed against the HIV-1 envelope glycoprotein can completely block HIV-1/SIV chimeric virus infections of macaque monkeys. Nat Med 1999;5:204–10.
[12] Mascola JR, Stiegler G, VanCott TC, Katinger H, Carpenter CB, Hanson CE, et al. Protection of macaques against vaginal transmission of a pathogenic HIV-1/SIV chimeric virus by passive infusion of neutralizing antibodies. Nat Med 2000;6:207–10.
[13] Parren PW, Marx PA, Hessell AJ, Luckay A, Harouse J, Cheng-Mayer C, et al. Antibody protects macaques against vaginal challenge with a pathogenic R5 simian/human immunodeficiency virus at serum levels giving complete neutralization in vitro. J Virol 2001;75:8340–7.
[14] Borrow P, Lewicki H, Hahn BH, Shaw GM, Oldstone MB. Virus-specific CD8+ cytotoxic T-lymphocyte activity associated with control of viremia in primary human immunodeficiency virus type 1 infection. J Virol 1994;68:6103–10.
[15] Ogg GS, Jin X, Bonhoeffer S, Dunbar PR, Nowak MA, Monard S, et al. Quantitation of HIV-1-specific cytotoxic T lymphocytes and plasma load of viral RNA. Science 1998;279:2103–6.
[16] Matano T, Shibata R, Siemon C, Connors M, Lane HC, Martin MA. Administration of an anti-CD8 monoclonal antibody interferes with the clearance of chimeric simian/human immunodeficiency virus during primary infections of rhesus macaques. J Virol 1998;72:164–9.
[17] Schmitz JE, Kuroda MJ, Santra S, Sasseville VG, Simon MA, Lifton MA, et al. Control of viremia in simian immunodeficiency virus infection by CD8+ lymphocytes. Science 1999;283:857–60.
[18] McMichael AJ, Hanke T. HIV vaccines 1983–2003. Nat Med 2003;9:874–80.
[19] Verschoor EJ, Mooij P, Oostermeijer H, van der Kolk M, ten Haaft P, Verstrepen B, et al. Comparison of immunity generated by nucleic acid-MF59-, and ISCOM-formulated human immunodeficiency virus type 1 vaccines in Rhesus macaques: evidence for viral clearance. J Virol 1999;73:3292–300.
[20] Yoshino N, Lu FX, Fujihashi K, Hagiwara Y, Kataoka K, Lu D, et al. A novel adjuvant for mucosal immunity to HIV-1 gp120 in nonhuman primates. J Immunol 2004;173:6850–7.
[21] Koopman G, Bogers WM, van Gils M, Koornstra W, Barnett S, Morein B, et al. Comparison of intranasal with targeted lymph node immunization using PR8-Flu ISCOM adjuvanted HIV antigens in macaques. J Med Virol 2007;79:474–82.
[22] Barnett SW, Srivastava IK, Kan E, Zhou F, Goodsell A, Cristillo AD, et al. Protection of macaques against vaginal SHIV challenge by systemic or mucosal and systemic vaccinations with HIV-envelope. AIDS 2008;22:339–48.
[23] Flynn NM, Forthal DN, Harro CD, Judson FN, Mayer KH, Para MF, et al. Placebo-controlled phase 3 trial of a recombinant glycoprotein 120 vaccine to prevent HIV-1 infection. J Infect Dis 2005;191:654–65.
[24] Bogers WM, Cheng-Mayer C, Montelaro RC. Developments in preclinical AIDS vaccine efficacy models. AIDS 2000;14:141–51.
[25] Akagi T, Kawamura M, Ueno M, Hiraishi K, Adachi M, Serizawa T, et al. Mucosal immunization with inactivated HIV-1-capturing nanospheres induces a significant HIV-1-specific vaginal antibody response in mice. J Med Virol 2003;69:163–72.
[26] Akagi T, Ueno M, Hiraishi K, Baba M, Akashi M. AIDS vaccine: intranasal immunization using inactivated HIV-1-capturing core-corona type polymeric nanospheres. J Control Release 2005;109:49–61.
[27] Wang X, Akagi T, Akashi M, Baba M. Development of core-corona type polymeric nanoparticles as an anti-HIV-1 vaccine. Mini-Rev Org Chem 2007;4:281–90.
[28] Miyake A, Akagi T, Enose Y, Ueno M, Kawamura M, Horiuchi R, et al. Induction of HIV-specific antibody response and protection against vaginal SHIV transmission by intranasal immunization with inactivated SHIV-capturing nanospheres in macaques. J Med Virol 2004;73:368–77.
[29] Akagi T, Baba M, Akashi M. Preparation of nanoparticles by the self-organization of polymers consisting of hydrophobic and hydrophilic segments: potential applications. Polymer 2007;48:6729–47.
[30] Matsusaki M, Hiwatari K, Higashi M, Kaneko T, Akashi M. Stably-dispersed and surface-functional bionanoparticles prepared by self-assembling amphipathic polymers of hydrophilic poly(γ-glutamic acid) bearing hydrophobic amino acids. Chem Lett 2004;33:398–9.
[31] Akagi T, Kaneko T, Kida T, Akashi M. Preparation and characterization of biodegradable nanoparticles based on poly(γ-glutamic acid) with L-phenylalanine as a protein carrier. J Control Release 2005;108:226–36.
[32] Akagi T, Kaneko T, Kida T, Akashi M. Multifunctional conjugation of proteins on/into core-shell type nanoparticles prepared by amphiphilic poly(γ-glutamic acid). J Biomater Sci Polym Ed 2006;17:875–92.
[33] Kim H, Akagi T, Akashi M. Preparation of size tunable amphiphilic poly(amino acid) nanoparticles. Macromol Biosci 2009;9:842–8.
[34] Uto T, Wang X, Sato K, Haraguchi M, Akagi T, Akashi M, et al. Targeting of antigen to dendritic cells with poly(γ-glutamic acid) nanoparticles induces antigen-specific humoral and cellular immunity. J Immunol 2007;178:2979–86.
[35] Akagi T, Wang X, Uto T, Baba M, Akashi M. Protein direct delivery to dendritic cells using nanoparticles based on amphiphilic poly(amino acid) derivatives. Biomaterials 2007;28:3427–36.
[36] Wang X, Uto T, Akagi T, Akashi M, Baba M. Induction of potent CD8+ T-cell responses by novel biodegradable nanoparticles carrying human immunodeficiency virus type 1 gp120. J Virol 2007;81:10009–16.
[37] Wang X, Uto T, Akagi T, Akashi M, Baba M. Poly(γ-glutamic acid) nanoparticles as an efficient antigen delivery and adjuvant system: potential for an AIDS vaccine. J Med Virol 2008;80:11–9.
[38] Joag SV, Li Z, Foresman L, Stephens EB, Zhao LJ, Adany I, et al. Chimeric simian/human immunodeficiency virus that causes progressive loss of CD4+ T cells and AIDS in pig-tailed macaques. J Virol 1996;70:3189–97.
[39] Suryanarayana K, Wiltrout TA, Vasquez GM, Hirsch VM, Lifson JD. Plasma SIV RNA viral load determination by real-time quantification of product generation in reverse transcriptase-polymerase chain reaction. AIDS Res Hum Retroviruses 1998;14:183–9.
[40] Peek LJ, Middaugh CR, Berkland C. Nanotechnology in vaccine delivery. Adv Drug Deliv Rev 2008;60:915–28.
[41] Matsuo K, Yoshikawa T, Oda A, Akagi T, Akashi M, Okada N, et al. Efficient generation of antigen-specific cellular immunity by vaccination with poly(γ-glutamic acid) nanoparticles entrapping endoplasmic reticulum-targeted peptides. Biochem Biophys Res Commun 2007;362:1069–72.
[42] Okamoto S, Yoshii H, Akagi T, Akashi M, Ishikawa T, Okuno Y, et al. Influenza hemagglutinin vaccine with poly(γ-glutamic acid) nanoparticles enhances the protection against influenza virus infection through both humoral and cell-mediated immunity. Vaccine 2007;25:8270–8.
[43] Okamoto S, Yoshii H, Ishikawa T, Akagi T, Akashi M, Takahashi M, et al. Single dose of inactivated Japanese encephalitis vaccine with poly(γ-glutamic acid) nanoparticles provides effective protection from Japanese encephalitis virus. Vaccine 2008;26:589–94.
[44] Yoshikawa T, Okada N, Oda A, Matsuo K, Matsuo K, Mukai Y, et al. Development of amphiphilic γ-PGA-nanoparticle based tumor vaccine: potential of the nanoparticulate cytosolic protein delivery carrier. Biochem Biophys Res Commun 2008;366:408–13.
[45] Yoshikawa T, Okada N, Oda A, Matsuo K, Matsuo K, Kayamuro H, et al. Nanoparticles built by self-assembly of amphiphilic poly(γ-glutamic acid) can deliver antigens to antigen-presenting cells with high efficiency: a new tumor-vaccine carrier for eliciting effector T cells. Vaccine 2008;26:1303–13.
[46] Uto T, Wang X, Akagi T, Zenkyu R, Akashi M, Baba M. Improvement of adaptive immunity by antigen-carrying biodegradable nanoparticles. Biochem Biophys Res Commun 2009;379:600–4.
[47] Uto T, Akagi T, Hamasaki T, Akashi M, Baba M. Modulation of innate and adaptive immunity by biodegradable nanoparticles. Immunol Lett 2009;125:46–52.
[48] Okamoto S, Matsuura M, Akagi T, Akashi M, Tanimoto T, Ishikawa T, et al. Poly(γ-glutamic acid) nano-particles combined with mucosal influenza virus hemagglutinin vaccine protects against influenza virus infection in mice. Vaccine 2009;27:5896–905.
[49] Akagi T, Higashi M, Kaneko T, Kida T, Akashi M. Hydrolytic and enzymatic degradation of nanoparticles based on amphiphilic poly(γ-glutamic acid)-*graft*-L-phenylalanine copolymer. Biomacromolecules 2006;7:297–303.
[50] Imaoka K, Miller CJ, Kubota M, McChesney MB, Lohman B, Yamamoto M, et al. Nasal immunization of nonhuman primates with simian immunodeficiency virus p55gag and cholera toxin adjuvant induces Th1/Th2 help for virus-specific immune responses in reproductive tissues. J Immunol 1998;161:5952–8.
[51] Egan MA, Chong SY, Hagen M, Megati S, Schadeck EB, Piacente P, et al. A comparative evaluation of nasal and parenteral vaccine adjuvants to elicit systemic and mucosal HIV-1 peptide-specific humoral immune responses in cynomolgus macaques. Vaccine 2004;22:3774–88.
[52] Mooij P, van der Kolk M, Bogers WM, ten Haaft PJ, Van Der Meide P, Almond N, et al. A clinically relevant HIV-1 subunit vaccine protects rhesus macaques from in vivo passaged simian-human immunodeficiency virus infection. AIDS 1998;12:15–22.
[53] Earl PL, Sugiura W, Montefiori DC, Broder CC, Lee SA, Wild C, et al. Immunogenicity and protective efficacy of oligomeric human immunodeficiency virus type 1 gp140. J Virol 2001;75:645–53.
[54] Robinson Jr WE, Kawamura T, Gorny MK, Lake D, Xu JY, Matsumoto Y, et al. Human monoclonal antibodies to the human immunodeficiency virus type 1 (HIV-1) transmembrane glycoprotein gp41 enhance HIV-1 infection in vitro. Proc Natl Acad Sci USA 1990;87:3185–9.
[55] Takeda A, Robinson JE, Ho DD, Debouck C, Haigwood NL, Ennis FA. Distinction of human immunodeficiency virus type 1 neutralization and infection enhancement by human monoclonal antibodies to glycoprotein 120. J Clin Invest 1992;89:1952–7.
[56] Douek DC, Brenchley JM, Betts MR, Ambrozak DR, Hill BJ, Okamoto Y, et al. HIV preferentially infects HIV-specific CD4+ T cells. Nature 2002;417:95–8.
[57] Kiepiela P, Ngumbela K, Thobakgale C, Ramduth D, Honeyborne I, Moodley E, et al. CD8+ T-cell responses to different HIV proteins have discordant associations with viral load. Nat Med 2007;13:46–53.
[58] Staprans SI, Barry AP, Silvestri G, Safrit JT, Kozyr N, Sumpter B, et al. Enhanced SIV replication and accelerated progression to AIDS in macaques primed to mount a CD4 T cell response to the SIV envelope protein. Proc Natl Acad Sci USA 2004;101:13026–31.
[59] Tsukamoto T, Takeda A, Yamamoto T, Yamamoto H, Kawada M, Matano T. Impact of cytotoxic-T-lymphocyte memory induction without virus-specific CD4+ T-Cell help on control of a simian immunodeficiency virus challenge in rhesus macaques. J Virol 2009;83:9339–46.

Virology 399 (2010) 134–143

Contents lists available at ScienceDirect

Virology

journal homepage: www.elsevier.com/locate/yviro

In vivo analysis of a new R5 tropic SHIV generated from the highly pathogenic SHIV-KS661, a derivative of SHIV-89.6

Kenta Matsuda, Katsuhisa Inaba, Yoshinori Fukazawa, Megumi Matsuyama, Kentaro Ibuki, Mariko Horiike, Naoki Saito, Masanori Hayami, Tatsuhiko Igarashi, Tomoyuki Miura *

Laboratory of Primate Model, Experimental Research Center for Infectious Diseases, Institute for Virus Research, Kyoto University, 53 Shogoinkawaramachi, Sakyo-ku, Kyoto 606-8507, Japan

ARTICLE INFO

Article history:
Received 9 November 2009
Returned to author for revision
14 December 2009
Accepted 5 January 2010
Available online 27 January 2010

Keywords:
AIDS
SHIV
CCR5 tropic
Mutagenesis
V3 region

ABSTRACT

Although X4 tropic SHIVs have been studied extensively, they show distinct infection phenotypes from those of R5 tropic viruses, which play an important role in HIV-1 transmission and pathogenesis. To augment the variety of R5 tropic SHIVs, we generated a new R5 tropic SHIV from the highly pathogenic X4 tropic SHIV-KS661, a derivative of SHIV-89.6. Based on consensus amino acid alignment analyses of subtype B R5 tropic HIV-1, five amino acid substitutions in the third variable region successfully changed the secondary receptor preference from X4 to R5. Improvements in viral replication were observed in infected rhesus macaques after two passages, and reisolated virus was designated SHIV-MK38. SHIV-MK38 maintained R5 tropism through *in vivo* passages and showed robust replication in infected monkeys. Our study clearly demonstrates that a minimal number of amino acid substitutions in the V3 region can alter secondary receptor preference and increase the variety of R5 tropic SHIVs.

Introduction

Simian immunodeficiency virus (SIV) macaque models for AIDS have been used extensively to elucidate the pathogenesis of human immunodeficiency virus type 1 (HIV-1) infection. Although SIV is an excellent model virus that has contributed to various virological discoveries, SIV has many limitations as an HIV-1 model. Because the antigenicity of SIV is different from that of HIV-1, it is difficult to evaluate HIV-1 vaccines in animal models by employing SIV as a challenge virus. This is especially true for evaluating the induction of neutralizing antibodies by HIV-1 vaccine candidates (Baba et al., 2000; Dey et al., 2009; Mascola et al., 2000). In addition to CCR5, SIV utilizes secondary receptors such as GPR1, GPR15 (Bob), and STRL-33 (Bonzo), which are scarcely used by HIV-1 (Clapham and McKnight, 2002). Although there have been no reports that have directly demonstrated the significance of these receptors for *in vivo* pathogenesis, possible influences of these minor receptors cannot be denied.

To supplement the limitations of the SIV model, a simian and human immunodeficiency virus (SHIV) macaque model has been generated. SHIVs were constructed by exchanging the envelope gene and other accessory genes of SIV with that of HIV-1 (Shibata et al., 1991). Therefore, SHIVs share the same envelope antigenicity and receptor usage with HIV-1. In early studies of HIV-1, isolated viruses were mostly X4 or dual tropic because they were isolated from AIDS patients using T-cell lines expressing CXCR4. Because envelope genes from X4 or dual tropic viruses were introduced to generate the chimeric virus, most SHIVs utilize CXCR4 as a secondary receptor. X4 tropic viruses infect distinct subsets of lymphocytes and the mode of viral replication during the acute phase of infection is different from that of R5 tropic viruses (Nishimura et al., 2004). During the acute phase of infection, X4 tropic SHIVs rapidly deplete circulating CD4 positive (+) T cells (Reimann et al., 1996; Sadjadpour et al., 2004). Most infected monkeys fail to seroconvert, because rapid depletion of helper T cells typically occurs within 4 weeks of infection. In contrast, R5 tropic viruses do not show such a catastrophic reduction in CD4+ T cells. The phenotypes observed during X4 SHIV infection are rare during actual HIV-1 infection, and it has been suggested that R5 tropic viruses are mainly involved in HIV-1 transmission and pathogenesis (Margolis and Shattock, 2006). Therefore, there is a demand for R5 tropic SHIVs in this field of research.

There are some R5 tropic SHIVs that have already been used in various experiments, including analyses on the efficacy of broadly neutralizing antibodies (Hessell et al., 2009). Due to the paucity of available R5 tropic SHIVs, however, it is difficult to conduct comparative analyses on the efficacy of neutralizing antibodies between different strains of SHIVs. *In vivo* analyses of neutralizing antibodies should be conducted with more than one or even a mixture of several strains of R5 tropic virus to reflect the wide variety of HIV-1 envelope genes that are found worldwide. Therefore, our primary aim

* Corresponding author. Mailing address: Laboratory of Primate Model, Experimental Research Center for Infectious Diseases, Institute for Virus Research, Kyoto University, 53 Shogoinkawaramachi, Sakyo-ku, Kyoto 606-8507, Japan. Fax: +81 75 761 9335.
E-mail address: tmiura@virus.kyoto-u.ac.jp (T. Miura).

0042-6822/$ - see front matter © 2010 Elsevier Inc. All rights reserved.
doi:10.1016/j.virol.2010.01.008

was to generate a new R5 tropic SHIV, which carries a different *env* from that of other existing R5 SHIVs.

Currently available R5 SHIVs were constructed by introducing the envelope gene and other accessory genes from R5 tropic HIV-1 into the SIV backbone (Humbert et al., 2008; Luciw et al., 1995). There is one report that demonstrated the construction of an R5 tropic SHIV by exchanging the whole third variable region (V3) of an X4 tropic SHIV with that of an R5 SHIV (Ho et al., 2005). This study clearly indicated that the V3 region of the envelope gene determines the secondary receptor preference *in vivo*. Although other studies have indicated that there are specific amino acids within the V3 region that are responsible for receptor preference (Cardozo et al., 2007; Yamaguchi-Kabata et al., 2004), there have been no reports demonstrating the generation of R5 tropic SHIV by the introduction of specific amino acid substitutions to the V3 region. Therefore, our secondary aim in this study was to alter the receptor usage of a well-studied X4 tropic SHIV by introducing a minimal number of amino acid substitutions in the *env* V3 region. The consensus amino acid alignment of subtype B R5 tropic HIV-1, which is strongly correlated with secondary receptor usage (Cardozo et al., 2007; Yamaguchi-Kabata et al., 2004), was introduced to the V3 region of a highly pathogenic SHIV-KS661 that possesses the typical infection phenotype of X4 tropic SHIV (Fukazawa et al., 2008; Miyake et al., 2006). SHIV-KS661 is a molecular clone constructed from the consensus sequence of SHIV-C2/1 (Gen Bank accession number AF21718) (Shinohara et al., 1999), a derivative of the non-pathogenic SHIV-89.6

Results

Generation of R5 tropic SHIV-MK1 from the highly pathogenic X4 tropic SHIV-KS661

The X4 tropic virus SHIV-KS661, a derivative of SHIV-89.6, depletes CD4+ T lymphocytes in systemic tissues within weeks of infection and causes AIDS-like symptoms in macaque monkeys (Fukazawa et al., 2008; Miyake et al., 2006). To convert the virus into an R5 tropic virus, we introduced five amino acid substitutions in the V3 region of SHIV-KS661 by site-directed mutagenesis. The positions of the substitutions were selected using information from alignment of the V3 amino acids of R5 tropic HIV-1 (Cardozo et al., 2007; Yamaguchi-Kabata et al., 2004). All five substitutions (E305K, R306S, R318T, R319G, and N320D) were accompanied by changes in electrical charge. As a result, the net charge of the V3 region shifted towards being more acidic (Fig. 1A). To determine whether this mutant, designated SHIV-MK1, was capable of replication within monkey cells, we spinoculated SHIV-MK1 on rhPBMCs at an MOI of 0.1. The RT activity in the supernatant was monitored daily. The X4 tropic SHIV-DH12R-CL-7 and parental SHIV-KS661 actively replicated on rhPBMCs, reaching its peak RT activity level 4 days after inoculation. The R5 tropic SIVmac239 reached its peak RT value at the same time point; however, the peak value was less than 50% of that of SHIV-DH12R-CL-7 and SHIV-KS661. SHIV-MK1 also replicated on rhPBMCs, but it took 2 days longer to reach peak RT activity levels, and the peak RT value was significantly lower than that of the parental SHIV-KS661 (Fig. 1B).

Next, to determine whether SHIV-MK1 was capable of utilizing CCR5, but not CXCR4, we conducted a small molecule inhibitor assay. Briefly, SIVmac239, SHIV-DH12R-CL-7, SHIV-KS661, or SHIV-MK1 was spinoculated on rhPBMCs that were preincubated with AD101 (R5 inhibitor), AMD3100 (X4 inhibitor), or both inhibitors at various concentrations. The supernatant RT activities were measured 5 days post-inoculation. The replication of X4 tropic SHIV-DH12-CL-7 was inhibited with AMD3100 in a dose-dependent manner; however, it was not restrained with AD101 as described previously (Igarashi et al., 1999, 2003; Sadjadpour et al., 2004). The same pattern was observed in SHIV-KS661-infected rhPBMCs, thus indicating that this virus is also an X4 tropic virus. In contrast, there was no replication inhibition of R5 tropic SIVmac239 in the presence of AMD3100; however, dose-dependent inhibition was observed in the presence of AD101. This result is consistent with other reports (Marcon et al., 1997; Zhang et al., 2000). SHIV-MK1 exhibited the same inhibition profile as SIVmac239, indicating that this virus predominantly utilizes CCR5, but not CXCR4, as an entry secondary receptor.

R5 tropic SHIV-MK1 can replicate in rhesus macaques

To determine whether SHIV-MK1 is capable of replication in rhesus macaques, we intravenously inoculated two monkeys (MM482 and MM483) with 20,000 TCID50 SHIV-MK1. Large amount of virus was inoculated to this group of monkey because *in vitro* replication of SHIV-MK1 was significantly weak compared with that of parental SHIV-KS661. As a control, two other monkeys (MM455 and MM459) were infected with 2000 TCID50 SHIV-KS661, a sufficient amount of virus to induce AIDS-like symptoms (Fukazawa et al., 2008; Miyake et al., 2006). Plasma viral RNA loads were monitored periodically using quantitative RT-PCR. Both groups of infected monkeys exhibited viremia, which reached peak plasma viral RNA loads of 10^6–10^8 copies/ml 2 weeks post-infection. In SHIV-KS661-infected monkeys, the set point of plasma viral RNA loads was between 10^4 and 10^6 copies/ml (Fig. 2Ai). In contrast, the plasma viral RNA load in one of the two monkeys infected with SHIV-MK1 was undetectable by 6 weeks post-infection, although 10-fold more virus was inoculated. The other monkey maintained 10^3–10^4 copies/ml plasma viral RNA for more than 25 weeks post-infection (Fig. 2Aii).

Next, circulating CD4+ T lymphocytes were analyzed by fluorescence activated cell sorting (FACS) to elucidate the impact of infection on lymphocyte subsets. As previously reported, X4 tropic SHIV-KS661 caused a massive depletion of circulating CD4+ T lymphocytes within 4 weeks post-infection (Fig. 2Bi). In contrast, circulating CD4+ T lymphocytes transiently decreased in monkeys infected with SHIV-MK1; however, they tended to recover by 24 weeks post-infection (Fig. 2Bii).

Because X4 tropic viruses preferably target naive CD4+ T lymphocytes, and R5 tropic viruses preferably target memory CD4+ T lymphocytes, circulating memory and naive CD4+ T lymphocytes were analyzed. The ratios of memory and naive CD4+ T cells were monitored 0, 2, 4, and 8 weeks post-SHIV-MK1 infection (Fig. 2C). Consistent with previous reports (Nishimura et al., 2004), X4 tropic SHIV-KS661 preferentially depleted naive T lymphocytes by 2 weeks post-infection. Although there was a subtle reduction in CD4+ T lymphocytes, the ratio of memory and naive CD4+ T lymphocytes did not change in SHIV-MK1-infected monkeys. This result indicates that a reduction in CD4+ T cells during SHIV-MK1 infection was not sufficient to alter the ratio of memory T cells, at least in circulating T lymphocytes.

The intestine is an effecter site where most CD4+ T lymphocytes are memory cells, and is the primary target for R5 tropic viruses (Harouse et al., 1999; Veazey et al., 1998). To elucidate the impact of viral infection in the intestine, tissue samples from the jejunum were obtained periodically and CD4+ T lymphocyte subsets were analyzed (Fig. 2D). As reported previously, CD4+ T lymphocytes of KS661-infected monkeys were depleted by 4 weeks post-infection (Fukazawa et al., 2008; Miyake et al., 2006). Although CD4+ T lymphocyte depletion was observed in one of the SHIV-MK1-infected monkeys (MM482) within 4 weeks post-infection, CD4+ T lymphocytes recovered as plasma viral RNA loads decreased. Another SHIV-MK1 infected monkey (MM483) whose plasma viral RNA load dropped below detectable levels showed only a transient reduction in CD4+ lymphocytes 5 weeks after infection. Taken together, these results suggest that, although the magnitude of jejunal CD4+ T-cell reduction was greater than that of circulating CD4+ T cells, the capability of SHIV-MK1 to cause CD4+ T lymphocyte depletion in the jejunum is not as strong as the parental SHIV-KS661.

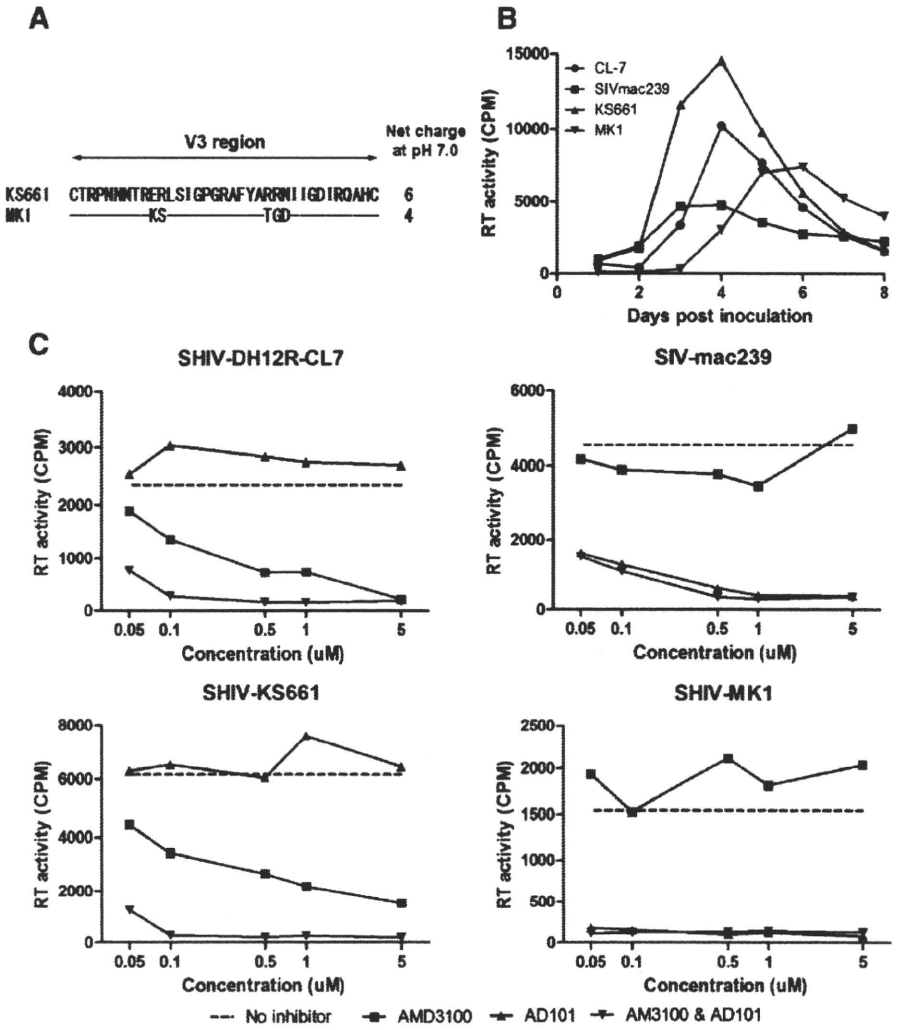

Fig. 1. Construction and *in vitro* analysis of SHIV-MK1. (A) gp120 V3 amino acid alignment of SHIV-MK1. Amino acid substitution positions are indicated under the parental SHIV-KS661 alignment. The net charge at pH 7.0 is indicated beside each amino acid alignment. (B) SHIV and SIV replication in rhPBMCs. The replication of control viruses (SIVmac239, SHIV-DH12R-CL7, and SHIV-KS661) and the mutant virus (SHIV-MK1) are shown. Culture supernatants were collected at the indicated time points, and RT activity was determined. Representative results of three independent experiments are shown. (C) Secondary receptor inhibitor sensitivity of the three SHIV inocula and an SIV control. The inoculum viruses SHIV-DH12R-CL7, SIVmac239, SHIV-KS661, and SHIV-MK1 were spinoculated on rhPBMCs in the presence of the indicated small molecule inhibitors. The inhibitor concentrations used were 0.05, 0.1, 0.5, 1, and 5 μM. The RT activity on day 5 post-infection was determined by the absence (dashed line) or presence of an inhibitor in the medium.

In vivo passage and characterization of the reisolated virus, SHIV-MK38

To adapt SHIV-MK1, we conducted *in vivo* passages. Briefly, disaggregated lymphocytes from inguinal lymph nodes and fresh blood collected from SHIV-MK1-infected MM482, were mixed and intravenously inoculated into an uninfected monkey, MM498. During the first passage, MM498 showed a plasma viral RNA load peak and set point equal to that of SHIV-MK1-infected MM482. During the second passage, disaggregated lymphocytes from inguinal lymph nodes and fresh blood collected from MM498 were mixed and intravenously inoculated into an uninfected monkey, MM504. MM504 showed a peak plasma viral RNA load of 5×10^7 copies/ml, which is slightly higher than that of MM482 and MM498. Furthermore, the set point of the viral load ranged from 10^4 to 10^6 copies/ml, which is approximately 10 times higher than that of MM482 and MM498 (Fig. 3A).

Although the inoculum doses were different in passaged monkeys, this result suggests that SHIV-MK1 acquired a better replicative capacity through *in vivo* passage. Therefore, we decided to reisolate the virus from MM504 for *in vitro* characterization. Briefly, CD8-depleted PBMCs from MM504 and an uninfected monkey were co-cultured for 2 weeks. The culture supernatant with the highest RT activity was stored in liquid nitrogen. This virus stock was designated SHIV-MK38.

First, we examined the replication kinetics of SHIV-MK38 in rhPBMCs. The infection assay revealed that although SHIV-MK38 could not replicate as fast or as efficiently as the parental KS661, there was a slight improvement in replication capacity compared with the original SHIV-MK1 (Fig. 3B). This result indicates that mutations that arose through *in vivo* passage increased replication ability in rhPBMCs.

As shown in Fig. 1B, however, X4 tropic viruses (SHIV-DH12R-CL-7 and SHIV-KS661) usually show fast and efficient replication in PBMCs compared with that of R5 tropic viruses (SIVmac239 and SHIV-MK1). Hence, there is the possibility of reversion in the V3 region, which may give SHIV-MK38 the appearance of having better replication capacity in rhPBMCs (Cho et al., 1998). Therefore, we examined the viral genome sequence to rule out the presence of reversions in the V3 region. Indeed, there were no back mutations in the V3 region of SHIV-MK38 when the V1 to V3 regions of the *env* sequences from 14

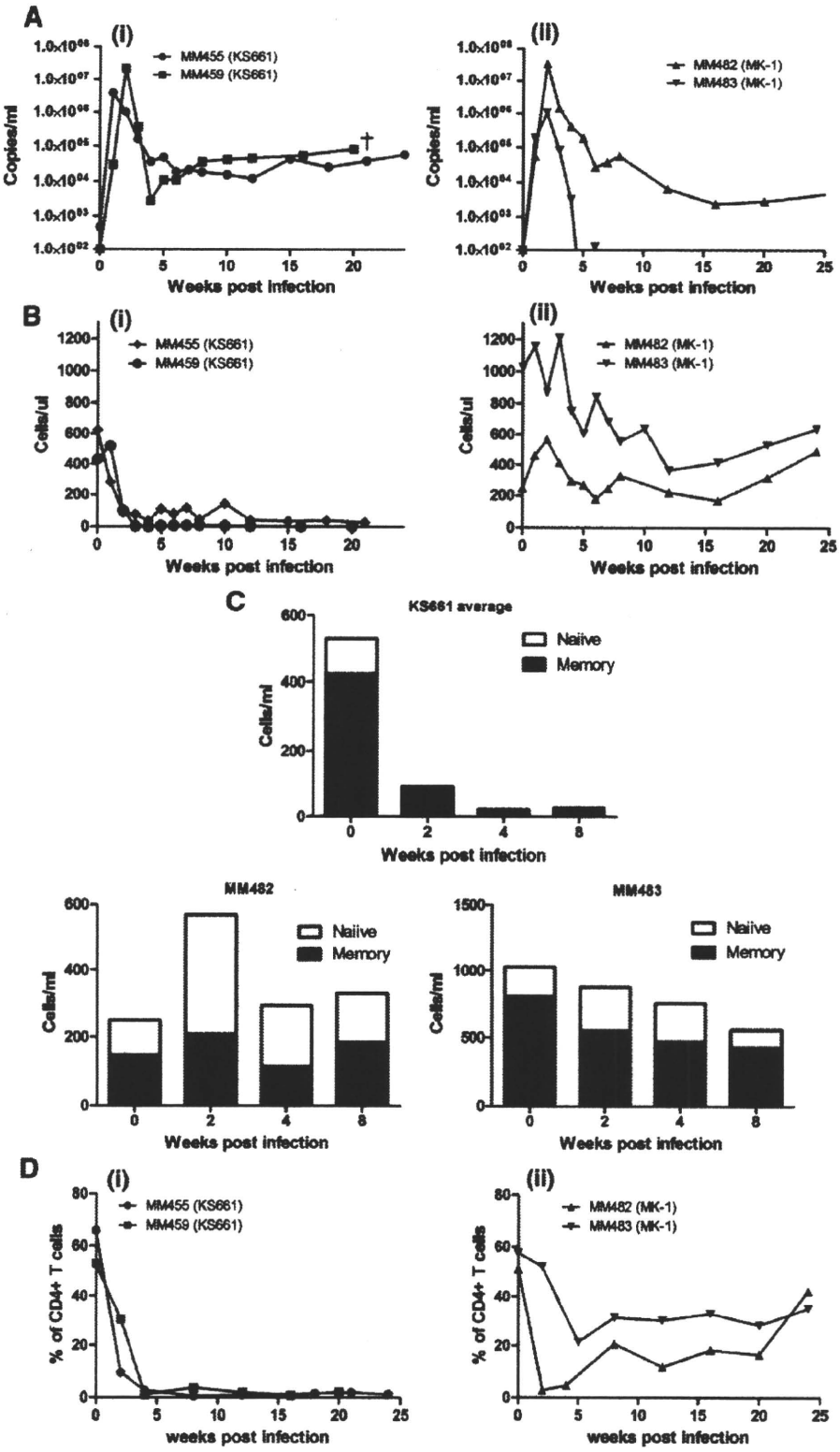

Fig. 2. *In vivo* replication of MK1. (A) Plasma viral RNA loads in SHIV-infected rhesus monkeys were measured at the indicated times. A total of 2000 TCID50 SHIV-KS661 was inoculated intravenously into MM455 and MM459 as a control group (i) and 20,000 TCID50 SHIV-MK1 was inoculated intravenously into MM482 and MM483 (ii). (B) CD4+ T lymphocytes were enumerated using FACS analysis in the SHIV-KS661 infected group (i) and the SHIV-MK1 infected group (ii) over the course of infection. (C) Changes in naive (open bar) and memory (black bar) CD4+ T cells in rhesus macaques inoculated with SHIV-KS661 (average of two infected monkeys) and SHIV-MK1 (MM482 and MM483) 0, 2, 4, and 8 weeks post-inoculation. (D) Percentage of CD4+ T lymphocytes in the jejunum. Tissues from the jejunum were collected from SHIV-KS661 infected monkeys (i) and SHIV-MK1 infected monkeys (ii) with a pediatric enteroscope, and were analyzed by FACS.

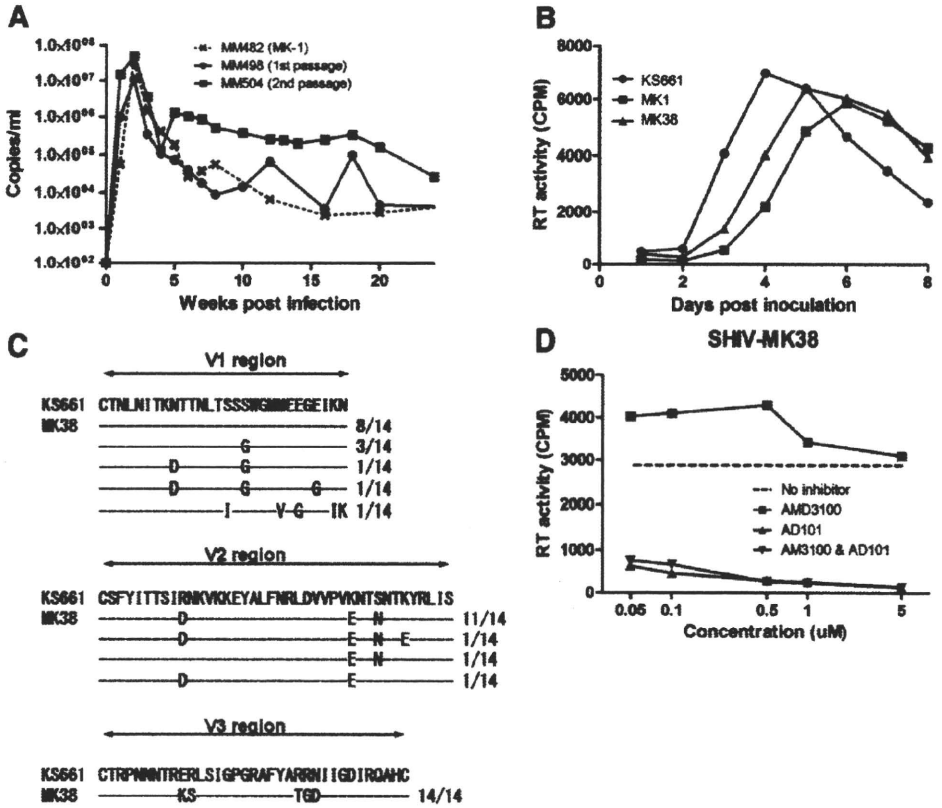

Fig. 3. *In vivo* adaptation of SHIV-MK1, and *in vitro* analysis of reisolated virus. (A) Plasma viral RNA loads of passaged monkeys were measured at the indicated times. The whole blood and dissociated lymph nodes from SHIV-MK1-infected MM482 were transfused into MM498 (first passage) 25 weeks post-inoculation. The whole blood and disaggregated lymph nodes from MM498 were transfused into MM504 (second passage) 5 weeks post-inoculation. (B) SHIV replication in rhPBMCs. The replication of control viruses (SHIV-KS661 and SHIV-MK1) and a passaged virus (SHIV-MK38) is shown. Culture supernatants were collected at the indicated time points, and RT activity was determined. Representative results of three independent experiments are shown. (C) gp120 V1, V2, and V3 amino acid alignment of SHIV-KS661 and 14 clones of SHIV-MK38. The positions of the amino acid substitutions in the 14 clones are indicated under the SHIV-KS661 sequence. (D) Secondary receptor inhibitor sensitivity of the SHIV-MK38 inoculum. RT activity 5 days post-infection was determined in the absence (dashed line) or presence of an inhibitor in the medium.

clones were analyzed (Fig. 3C). Nonetheless, we found mutations in the V1 and V2 regions of SHIV-MK38. These mutations have the potential to affect secondary receptor usage.

To confirm whether SHIV-MK38 maintains R5 tropism, we conducted a small molecule inhibitor assay, which revealed that SHIV-MK38 could not replicate in rhPBMCs in the presence of AD101 but could replicate in the presence of AMD3100. This indicates that SHIV-MK38 maintains R5 tropism in the primary cell (Fig. 3D).

In vivo analysis of SHIV-MK38

To evaluate whether SHIV-MK38-infected monkeys show stable infection phenotypes compared with that of SHIV-MK1-infected monkeys, we inoculated three monkeys with 20,000 TCID50 SHIV-MK38. All three infected monkeys possessed a peak plasma viral RNA load of approximately 10^7 copies/ml 12 days after infection. Although the peak plasma viral RNA load was at the same level in these monkeys, set points varied widely (Fig. 4A). That of MM501 was 10^3–10^4 copies/ml, which is similar to that of SHIV-MK1-infected MM482. MM502 had a slightly higher set point of 10^4–10^5 copies/ml, which is similar to that of MM504. Finally, MM481 had the highest set point, at 10^6–10^7 copies/ml. No monkey showed a decrease in viral RNA load under the detectable level, indicating that SHIV-MK38 robustly replicates in rhesus macaques.

Next, reductions in circulating CD4+ T cells were analyzed. Unlike SHIV-MK1 infection, all of the SHIV-MK38-infected monkeys exhibited a continuous reduction in CD4+ T cells without signs of recovery (Fig. 4B). The impact of infection on ratios of circulating memory and naive CD4+ T cells was also analyzed. Compared with monkeys infected with SHIV-MK1, SHIV-MK38 preferentially reduced memory fractions of CD4+ T cells (Figs. 2C and 4C).

To elucidate how improvements in viral replication affect the reduction of CD4+ T cells at effector sites, tissue samples from the jejunum were obtained periodically and CD4+ T lymphocyte subsets were analyzed. In SHIV-MK38-infected monkeys, CD4+ T cells were rapidly reduced by 2 weeks post-infection, as seen in SHIV-MK1 infection. Furthermore, recovery of CD4+ T cells was not observed in infected monkeys. In particular, CD4+ T cells in MM481 were depleted throughout the observation period (Figs. 2D and 4D). These data indicate that SHIV-MK38 has an increased ability to reduce CD4+ T cells and maintain higher plasma viral RNA loads in infected monkeys compared with pre-adapted SHIV-MK1.

Discussion

Based on the analysis of consensus amino acid alignments of subtype B R5 viruses, five amino acid substitutions (E305K, R306S, R318T, R319G, and N320D) were introduced into the V3 region of the pathogenic SHIV-KS661 *env* gene by site-directed mutagenesis. These substitutions included the 11/24/25th amino acid of the V3 region, which are strongly correlated with secondary receptor usage (Cardozo et al., 2007; Yamaguchi-Kabata et al., 2004). As expected, these substitutions successfully altered the secondary receptor usage of SHIV-KS661 from X4 to R5 tropic. This result clearly demonstrates

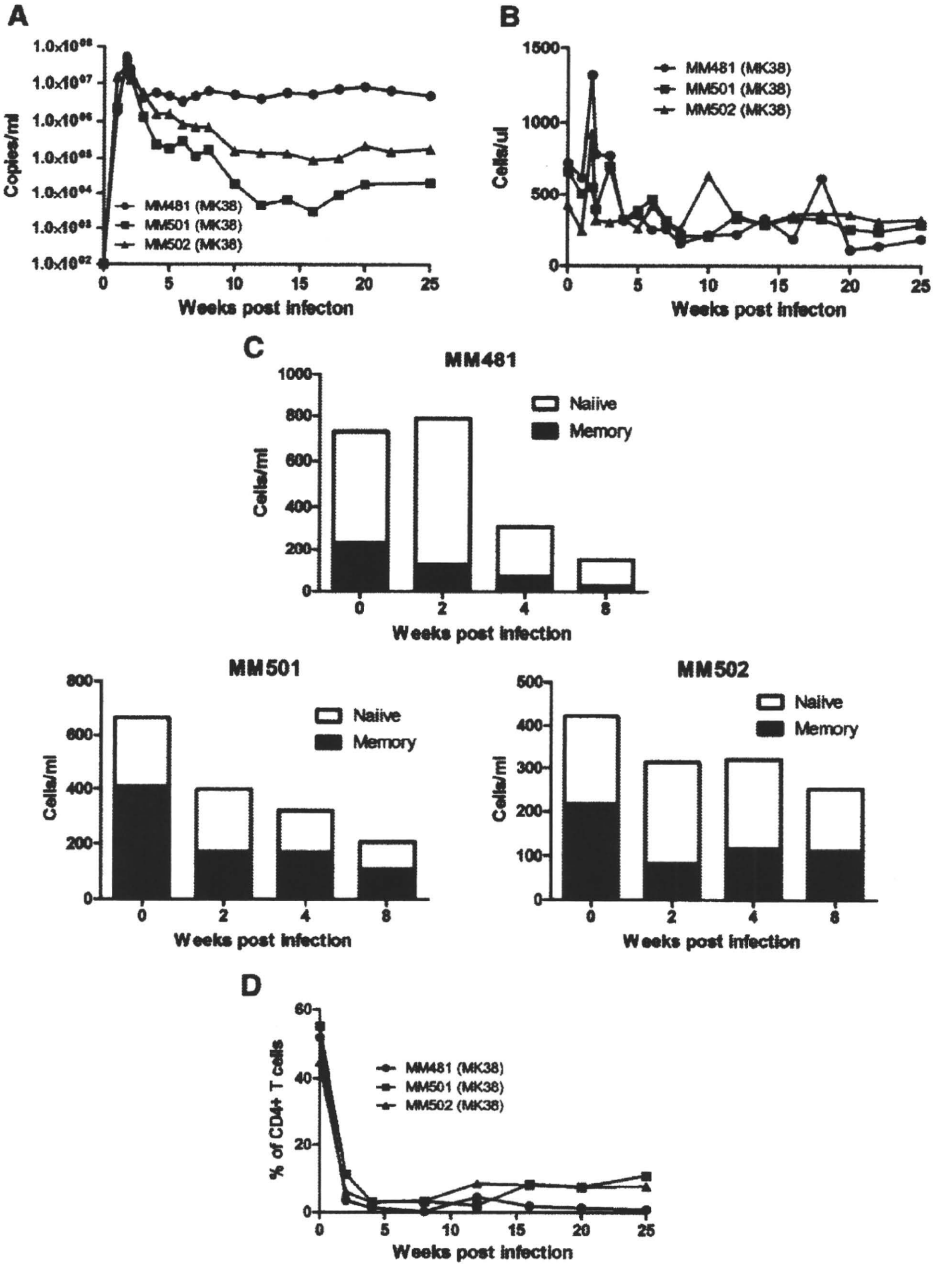

Fig. 4. *In vivo* replication of SHIV-MK38. (A) Plasma viral RNA loads in SHIV-infected rhesus monkeys were measured at the indicated times. A total of 20,000 TCID50 SHIV-MK38 were inoculated into MM481, MM501, and MM502. (B) CD4+ T lymphocytes were enumerated using FACS analysis in SHIV-MK38-infected monkeys over the course of infection. (C) Changes in naïve (open bar) and memory (filled bar) CD4+ T cells in rhesus macaques inoculated with SHIV-MK38 0, 2, 4, and 8 weeks post-inoculation. (D) Percentage of CD4+ T lymphocytes in the jejunum. Tissues from the jejunum were collected from SHIV-MK38-infected monkeys with a pediatric enteroscope, and analyzed by FACS.

for the first time that specific V3 amino acid alignment information from HIV-1 can be applied to SHIV to alter secondary receptor usage, at least in the context of the subtype B envelope. The prediction of viral secondary receptor tropism in HIV-1-infected people prior to the prescription of CCR5 antagonists has important economic and practical implications. There are at least six algorithms that predict viral tropism from the V3 sequence; however, the accuracy of these algorithms must be improved (de Mendoza et al., 2008; Dorr et al., 2005; Fätkenheuer et al., 2005; Mefford et al., 2008). For example, the Web PSSM algorithm (Jensen et al., 2003) predicts that SHIV-MK1 exclusively utilizes CCR5, while the Geno2pheno algorithm (Sing et al., 2007) suggests that it may also utilize CXCR4. In this study, we demonstrated that specific amino acids in the V3 region are responsible for secondary receptor usage both *in vitro* and *in vivo*. Accumulation of this type of information will provide important data that can be used to improve predictions and increase the genotype sensitivity of algorithms.

Although minimal numbers of amino acid substitutions were introduced to change secondary receptor usage, SHIV-MK1 showed relatively inefficient replication compared with that of parental SHIV-KS661, both *in vitro* and *in vivo*. SHIV-MK1 caused measurable levels of viremia in infected monkeys; however, plasma viral RNA levels dropped below detectable levels in one of two infected monkeys 6 weeks after inoculation, despite the fact that enormous amount of

virus was inoculated. When evaluating the efficacy of passively administered neutralizing antibodies, or those induced by candidate anti-HIV-1 vaccines, this variability in viral replication is not desirable for the assessment of efficacy, because it is impossible to determine whether the virus was controlled by natural immune responses or by vaccine-induced immune responses. However, an improvement in viral replication was observed in rhPBMCs after *in vivo* passage of SHIV-MK1. This outcome suggests that, as in the case of other existing R5 tropic SHIVs, *in vivo* adaptation is required regardless of the minimal number of amino acid substitutions (Humbert et al., 2008; Tan et al., 1999).

Because various reports have demonstrated the emergence of the X4 tropic virus from the R5 tropic virus after serial passages (Ho et al., 2007; Pastore et al., 2000), there was a concern over the emergence of the X4 tropic virus through two *in vivo* passages. Although there were only five amino acid substitutions, no reversions in any of the substituted amino acids in the V3 region were observed. Some mutations were accompanied by amino acid substitutions in V1 and V2 regions. Previous reports suggest that these two variable regions may influence secondary receptor preference (Cho et al., 1998); however, a small molecule inhibitor assay revealed that SHIV-MK38 maintained R5 tropism after passage. The V1 and V2 regions also play a role in sensitivity against neutralizing antibodies (Laird et al., 2008; Wei et al., 2003). Although further investigations are required, SHIV-MK38 could have developed mutations in the V1 and V2 regions to modify antigenicity in an attempt to evade neutralizing antibodies (Sagar et al., 2006). Indeed, neutralization assay on TZM-BL cells revealed that neutralizing antibody from an MK1-infected monkey can neutralize SHIV-KS661 and SHIV-MK1, but fail to neutralize SHIV-MK38. On the other hand, plasma from the monkey in which SHIV-MK38 was isolated could neutralize all three viruses. Thus, the antigenicity was changed through *in vivo* passages (Supplementary Figure). Taken together, these results suggest that the improved replication of SHIV-MK38 over MK1 was not due to the re-emergence of X4 tropic viruses. Furthermore, the acquisition of mutations outside the V3 region is most likely attributable to the improved replication of SHIV-MK38 *in vivo*.

To confirm the replication advantage of SHIV-MK38 over SHIV-MK1, SHIV-MK38 was intravenously inoculated into three uninfected monkeys. Despite the fact that the same amount of SHIV-MK38 was inoculated, higher peaks and set points of plasma RNA loads were observed in SHIV-MK38 compared with SHIV-MK1 infection. Although SHIV-MK38-infected monkeys showed no obvious signs of AIDS-like symptoms during the observation period, none of these monkeys was able to control viral replication. A greater reduction in the memory portion of circulating CD4+ T cells was observed in SHIV-MK38-infected monkeys. This preferential reduction of circulating memory CD4+ T cells was well defined in MM481, which correlates with the maintenance of high plasma viral RNA loads throughout the observation period. Reductions of CD4+ T cells in the jejunum of SHIV-MK38-infected monkeys were greater than that of SHIV-MK1-infected monkeys, and there was no obvious recovery during the observation period. These infection phenotypes are characteristic of an R5 tropic virus, which is distinct from the infection of X4 tropic SHIVs such as parental SHIV-KS661 (Fukazawa et al., 2008; Miyake et al., 2006).

Harous et al. clearly demonstrated that R5 tropic virus preferentially reduces mucosal CD4+ T cells where memory CD4+ T cells are abundant, whereas X4 tropic virus preferentially reduces peripheral CD4+ T cells where naive CD4+ T cells are abundant (Harouse et al., 1999). From this observation, it is clear that the receptor preference has strong impact on tissue specific CD4+ T-cell reductions. However, in some cases, systemic and irreversible reduction of CD4+ T cells was observed in highly pathogenic X4 SHIV infection (Fukazawa et al., 2008; Nishimura et al., 2004). It has been suggested that highly pathogenic X4 SHIV preferentially targets naive CD4+ T cells but eventually reduces memory CD4+ T cells (Nishimura et al., 2004). The depletion of CD4+ T cells at the effector site in SHIV-KS661 infected monkeys supports this suggestion (Fig. 2D).

The envelope gene of SHIV-MK38 belongs to subtype B, which can be compared with other subtype B or C R5 tropic SHIVs (Humbert et al., 2008; Tan et al., 1999). Comparing the efficacy of passively administered neutralizing antibodies and their induction by candidate HIV-1 vaccines against a variety of R5 tropic SHIVs would provide a more precise evaluation against a variety of HIV-1 strains worldwide (Wei et al., 2003). Furthermore, despite the fact that SHIV-MK38 is derived from SHIV-KS661, and mutations were obtained through the alteration of secondary receptor usage and passage, SHIV-MK38 is still genetically homologous to SHIV-89.6P, because they both originate from the same molecular clone, SHIV-89.6. Highly pathogenic X4 tropic SHIV-89.6P has been used extensively in various experiments, including vaccine concept evaluations (Shiver et al., 2002). There are claims, however, that the utilization of X4 tropic SHIVs as challenge viruses has led to overestimation of vector-based vaccines (Feinberg and Moore, 2002). Therefore, SHIV-MK38 can be useful in the future to determine whether such overestimations are truly caused by using X4 SHIVs or are due to using an SHIV derived from the specific lineage of SHIV-89.6.

Based on our observations, it can be concluded that R5 tropic SHIV-MK38 can robustly replicate, and we successfully generated a new R5 tropic SHIV by a new method. Although infected monkeys showed no signs of AIDS-like symptoms during the observation period, and further characterization such as neutralization profiles must be conducted, SHIV-MK38 has the potential to be a new R5 SHIV model.

Materials and methods

Virus production

Non-synonymous nucleotide substitutions in the V3 domain of the SHIV-KS661 *env* gene were introduced by site-directed mutagenesis for substitution of amino acids. A 5.9 kb DNA fragment containing the *env* V3 domain was subcloned into a pUC119 vector following digestion with restriction enzymes Sse8387I and XhoI. The resulting vector was designated pKS661v3, and was used as the template for two sets of polymerase chain reaction (PCR). All amplifications were performed as follows: one cycle of denaturation (98 °C, 5 min), 32 cycles of amplification (98 °C, 10 s/60 °C, 30 s/72 °C, 2 min), and an additional cycle for final extension (72 °C, 10 min) using iProof High-Fidelity Master Mix (Bio-Rad Laboratories, Hercules, CA). The following primers were used for the first set of PCR: 5′ CAATACAA-GAAAAAGTTTATCTATAGGACCAGGGAGAGCATTTTATGCAACAGGAGA-CATAATAGGAG 3′ (forward primer corresponding to the 7250–7317th nucleotides of SHIV-KS661; positions of mismatches are underlined) and 5′ GCTGAAGAGGCACAGGCTCCGC 3′ (reverse primer corresponding to the 8633–8612th nucleotide of SHIV-KS661; no mismatches). The following primers were used for the second set of PCR: 5′ CTCCTAT-TATGTCTCCTGTTGCATAAAATGCTCTCCCTGGTCCTATAGA-TAAACTTTTTCTTGTATTG 3′ (reverse primer corresponding to the 7317–7250th nucleotide of SHIV-KS661; positions of mismatches are underlined) and 5′ CTCCAGGACTAGCATAAATGG 3′ (forward primer corresponding to the 5617–5637th nucleotide of SHIV-KS661; no mismatches). The products from these two sets of PCR were mixed, and overlap PCR was performed using primers 5′ GCTGAAGAGGCA-CAGGCTCCGC 3′ and 5′ CTCCAGGACTAGCATAAATGG 3′. The PCR product was then digested with the restriction enzymes BsaBI and NcoI. The resulting fragment was introduced back into the pKS661v3 vector, and designated pKS661v3m. Then pKS661v3m DNA with mutations was digested by Sse8387I and XhoI, and the fragment was introduced back into the KS661 full genome plasmid, and designated pMK1.

SHIV-MK1 was prepared by transfecting pMK1 into the 293T cell line using the FuGENE 6 Transfection Reagent (Roche Diagnostics, Indianapolis, IN) and the culture supernatant 48 h after transfection, and was stored in liquid nitrogen until use. The same procedures were conducted to prepare SIVmac239 (Kestler et al., 1991), SHIV-KS661 (Shinohara et al., 1999), and SHIV-DH12R-CL7 (Igarashi et al., 1999). The 50% tissue culture infectious dose (TCID50) was measured using the C8166-CCR5 cell line (Shimizu et al., 2006).

Viral replication on rhPBMCs

Rhesus macaque PBMCs (rhPBMCs), prepared from an uninfected monkey, were suspended in Rosewell Park Memorial Institute (RPMI) 1640 medium supplemented with 10% (vol/vol) fetal bovine serum (FBS), 2 mM L-glutamine, and 1 mM sodium pyruvate, and then stimulated for 20 h with 25 μg/ml Concanavalin A (Sigma-Aldrich, St. Louis, USA), followed by an additional 2-day cultivation with 100 units/ml IL-2 (Shionogi, Osaka, Japan). On day 3, 5×10^4 cells were dispensed into 96-well round-bottom plates in triplicate. The cells were then inoculated with virus at a multiplicity of infection (MOI) of 0.1 using the spinoculation method (O'Doherty et al., 2000). Virion-associated reverse transcriptase (RT) activity of the culture supernatant was monitored periodically (Willey et al., 1988).

Inhibition of viral replication by a small molecule inhibitor

A small molecule inhibitor assay was conducted as described previously (Igarashi et al., 2003), with minor modifications. Briefly, uninfected rhesus PBMCs were prepared as described above. On day 3, 5×10^4 cells were dispensed into 96-well round-bottom plates. Various concentrations (0, 0.05, 0.1, 0.5, 1, and 5 μM) of a small molecule CCR5-specific receptor antagonist (AD101 was provided by Dr. Julie Strizki, Schering Plough Research Institute, Kenilworth, NJ) (Trkola et al., 2002) and/or a CXCR4-specific receptor antagonist (AMD3100; Sigma-Aldrich, St. Louis, MO) (Donzella et al., 1998) were added to duplicate wells and incubated for 1 h at 37 °C. Then each test virus was spinoculated at $1200\times g$ for 1 h at an MOI of 0.1. On day 5 post-infection, virus replications were assessed by RT assay of the culture supernatants.

Virus inoculation

Indian-origin rhesus macaques were used in accordance with the institutional regulations approved by the Committee for Experimental Use of Nonhuman Primates of the Institute for Virus Research, Kyoto University, Kyoto, Japan. Monkeys were housed in a biosafety level 3 facility and all procedures were performed in this facility. Collection of blood, biopsies, and i.v. virus inoculations (2000 TCID50 of SHIV-KS661, 20000 TCID50 of SHIV-MK1, 20000 TCID50 of SHIV-MK38) were performed on monkeys under anesthetization with ketamine hydrochloride (Daiichi-Sankyo, Tokyo, Japan). Plasma viral RNA loads were determined by quantitative RT-PCR as described previously (Kozyrev et al., 2002). Plasma viral RNA loads under 100 copies/ml were characterized as undetectable levels.

Jejunal biopsy

Tissue samples from the jejunum were collected with a pediatric enteroscope (Olympus GIF type XP260N, Olympus Medical System Corp., Tokyo, Japan). Five pieces (samples) of fresh jejunal tissue were placed on a shaker for 2 h at room temperature in 40 ml RPMI 1640 medium containing 10% FBS and 0.01 g collagenase from *Clostridium histolyticum* (Sigma-Aldrich, St. Louis, MO). Disaggregated cells were filtered through glass wool loaded in a 20 ml disposable syringe. Cells were prepared from the filtrate by centrifugation at a speed of 1200 rpm for 10 min. Subsets of lymphocytes in the resuspended cells were analyzed by flow cytometry.

Flow cytometry

To analyze CD4+ T lymphocytes, whole blood and jejunal samples were stained with two fluorescently labeled mouse monoclonal antibodies, fluorescein isothiocyanate (FITC) conjugated anti-monkey CD3 (Clone FN-18, BioSource Intl, Camarillo, CA) and phycoerythrin (PE) conjugated anti-human CD4 (Clone Nu-TH/I; Nichirei, Tokyo, Japan). To analyze memory and naive CD4+ T lymphocytes, whole blood and jejunal samples were stained with three fluorescently labeled mouse monoclonal antibodies, FITC conjugated anti-human CD95 (Clone DX2; BD Pharmingen, Tokyo, Japan), PE conjugated anti-human CD28 (Clone CD28.2; Coulter Immunotech, Marseille, France), and allophycocyanin (APC) conjugated anti-human CD4 (Clone L200; BD Pharmingen). After hemolysis of whole blood and jejunal samples using a lysing solution (Beckton Dickinson, Franklin Lakes, NJ), each type of labeled lymphocyte was examined on a FACScalibur analyzer using Cellquest (BD Biosciences, San Jose, CA). CD95+$CD4^{high}$+ cells were considered memory T lymphocytes, and CD95-CD28+$CD4^{high}$+ cells were considered naive T lymphocytes (Pitcher et al., 2002). The absolute number of lymphocytes in the blood was determined using an automated blood counter, KX-21 (Sysmex, Kobe, Japan).

In vivo passage

Inguinal lymph nodes were aseptically collected from MM482 25 weeks after infection. The lymph nodes were minced with scissors, disaggregated using an 85-ml Bellco Tissue Sieve Kit (Bellco Glass, Inc., Vineland, NJ), and filtered through a 100-μm pore cell strainer (REF 35-2360, BD Falcon, Franklin Lakes, NJ). Filtrates were centrifuged and then washed four times with phosphate-buffered saline (PBS). These disaggregated cells were mixed with 2 ml frozen plasma (collected from the animal 8 weeks post-infection and stored at −80 °C) and 20 ml fresh blood from MM482, and then transfused into an uninfected monkey (MM498) intravenously. During the second passage, inguinal lymph nodes were aseptically collected from MM498 5 weeks after infection. The disaggregated inguinal lymph node was mixed with 2 ml frozen plasma (collected 2 weeks post-infection), 5×10^7 cells inguinal lymphocytes (collected 16 days post-infection and stored at −80 °C), and 15 ml fresh blood, and then transfused into an uninfected monkey (MM504).

Reisolation of virus

Fresh blood was obtained from the uninfected monkey, and PBMCs were isolated. These cells were incubated for 30 min with PE labeled anti-CD8 antibody (SK1 clone, BD Pharmingen), then washed once with PBS. Next, cells were incubated with anti-PE MACS beads (Miltenyi Biotec, Bergisch Gladbach, Germany), and CD8− cells were negatively selected with a magnetic column. CD8− PBMCs were cultured as described above.

On day 0, fresh blood was obtained from MM504 (16 weeks post-infection) and CD8 cells were depleted as described above. CD8+ cells were also depleted from frozen PBMCs (obtained from MM504 8 weeks post-infection and stored at −80 °C). These CD8− PBMCs from uninfected and infected monkeys were co-cultured in PBMC culture medium (described above) at a concentration of 2×10^6 cells/ml at 37 °C. Medium was replaced daily for 16 days and culture supernatants were stored at −80 °C. The culture supernatant with the highest RT value was stored in liquid nitrogen. This virus stock was designated SHIV-MK38.

Sequence of V1, V2, and V3 regions of SHIV-MK38

SHIV-MK38 viral stock was used as a template for RT-PCR to amplify the V1 to V3 regions of the *env* gene. The forward primer 5′ GTGTAAAATTAACCCCACTCTGTG 3′ and reverse primer 5′ TGGGAGGGGCATACATTGCTTTTCC 3′ were used for RT-PCR. The amplified DNA fragment was cloned into the pCR2.1 vector using a TA Cloning Kit (Invitrogen, Carlsbad, CA), and 14 clones were sequenced.

Acknowledgments

We thank Dr. Julie Strizki, Schering Plough Research Institute, for providing AD101. This work was supported, in part, by Research on Human Immunodeficiency Virus/AIDS in Health and Labor Sciences research grants from the Ministry of Health, Labor and Welfare, Japan, a grant-in-aid for scientific research from the Ministry of Education and Science, Japan, a research grant for health sciences focusing on drug innovation for AIDS from the Japan Health Sciences Foundation, and a grant from the Program for the Promotion of Fundamental Studies in Health Sciences of the National Institute of Biomedical Innovation (NIBIO) of Japan.

Appendix A. Supplementary data

Supplementary data associated with this article can be found, in the online version, at doi:10.1016/j.virol.2010.01.008.

References

Baba, T.W., Liska, V., Hofmann-Lehmann, R., Vlasak, J., Xu, W., Ayehunie, S., Cavacini, L.A., Posner, M.R., Katinger, H., Stiegler, G., Bernacky, B.J., Rizvi, T.A., Schmidt, R., Hill, L.R., Keeling, M.E., Lu, Y., Wright, J.E., Chou, T.C., Ruprecht, R.M., 2000. Human neutralizing monoclonal antibodies of the IgG1 subtype protect against mucosal simian–human immunodeficiency virus infection. Nat. Med. 6 (2), 200–206.

Cardozo, T., Kimura, T., Philpott, S., Weiser, B., Burger, H., Zolla-Pazner, S., 2007. Structural basis for coreceptor selectivity by the HIV type 1 V3 loop. AIDS Res. Hum. Retroviruses 23 (3), 415–426.

Cho, M.W., Lee, M.K., Carney, M.C., Berson, J.F., Doms, R.W., Martin, M.A., 1998. Identification of determinants on a dualtropic human immunodeficiency virus type 1 envelope glycoprotein that confer usage of CXCR4. J. Virol. 72 (3), 2509–2515.

Clapham, P.R., McKnight, A., 2002. Cell surface receptors, virus entry and tropism of primate lentiviruses. J. Gen. Virol. 83 (Pt 8), 1809–1829.

de Mendoza, C., Van Baelen, K., Poveda, E., Rondelez, E., Zahonero, N., Stuyver, L., Garrido, C., Villacian, J., Soriano, V., Spanish HIV Seroconverter Study Group, 2008. Performance of a population-based HIV-1 tropism phenotypic assay and correlation with V3 genotypic prediction tools in recent HIV-1 seroconverters. J. Acquir. Immune. Defic. Syndr. 48 (3), 241–244.

Dey, B., Svehla, K., Xu, L., Wycuff, D., Zhou, T., Voss, G., Phogat, A., Chakrabarti, B.K., Li, Y., Shaw, G., Kwong, P.D., Nabel, G.J., Mascola, J.R., Wyatt, R.T., 2009. Structure-based stabilization of HIV-1 gp120 enhances humoral immune responses to the induced co-receptor binding site. PLoS Pathog. 5 (5), e1000445.

Donzella, G.A., Schols, D., Lin, S.W., Este, J.A., Nagashima, K.A., Maddon, P.J., Allaway, G.P., Sakmar, T.P., Henson, G., De Clercq, E., Moore, J.P., 1998. AMD3100, a small molecule inhibitor of HIV-1 entry via the CXCR4 co-receptor. Nat. Med. 4, 72–77.

Dorr, P., Westby, M., Dobbs, S., Griffin, P., Irvine, B., Macartney, M., Mori, J., Rickett, G., Smith-Burchnell, C., Napier, C., Webster, R., Armour, D., Price, D., Stammen, B., Wood, A., Perros, M., 2005. Maraviroc (UK-427,857), a potent, orally bioavailable, and selective small-molecule inhibitor of chemokine receptor CCR5 with broad-spectrum anti-human immunodeficiency virus type 1 activity. Antimicrob. Agents. Chemother. 49 (11), 4721–4732.

Fätkenheuer, G., Pozniak, A.L., Johnson, M.A., Plettenberg, A., Staszewski, S., Hoepelman, A.I., Saag, M.S., Goebel, F.D., Rockstroh, J.K., Dezube, B.J., Jenkins, T.M., Medhurst, C., Sullivan, J.F., Ridgway, C., Abel, S., James, I.T., Youle, M., van der Ryst, E., 2005. Efficacy of short-term monotherapy with maraviroc, a new CCR5 antagonist, in patients infected with HIV-1. Nat. Med. 11 (11), 1170–1172 Epub 2005 Oct 5.

Feinberg, M.B., Moore, J.P., 2002. AIDS vaccine models: challenging challenge viruses. Nat. Med 8 (3), 207–210.

Fukazawa, Y., Miyake, A., Ibuki, K., Inaba, K., Saito, N., Motohara, M., Horiuchi, R., Himeno, A., Matsuda, K., Matsuyama, M., Takahashi, H., Hayami, M., Igarashi, T., Miura, T., 2008. Small intestine CD4+ T cells are profoundly depleted during acute simian–human immunodeficiency virus infection, regardless of viral pathogenicity. J. Virol. 82 (12), 6039–6044.

Harouse, J.M., Gettie, A., Tan, R.C., Blanchard, J., Cheng-Mayer, C., 1999. Distinct pathogenic sequela in rhesus macaques infected with CCR5 or CXCR4 utilizing SHIVs. Science 30 (284(5415)), 816–819.

Hessell, A.J., Rakasz, E.G., Poignard, P., Hangartner, L., Landucci, G., Forthal, D.N., Koff, W. C., Watkins, D.I., Burton, D.R., 2009. Broadly neutralizing human anti-HIV antibody 2G12 is effective in protection against mucosal SHIV challenge even at low serum neutralizing titers. PLoS Pathog. 5 (5), e1000433.

Ho, S.H., Shek, L., Gettie, A., Blanchard, J., Cheng-Mayer, C., 2005. V3 loop-determined coreceptor preference dictates the dynamics of CD4+-T-cell loss in simian–human immunodeficiency virus-infected macaques. J. Virol. 79 (19), 12296–12303.

Ho, S.H., Tasca, S., Shek, L., Li, A., Gettie, A., Blanchard, J., Boden, D., Cheng-Mayer, C., 2007. Coreceptor switch in R5-tropic simian/human immunodeficiency virus-infected macaques. J. Virol. 81 (16), 8621–8633.

Humbert, M., Rasmussen, R.A., Song, R., Ong, H., Sharma, P., Chenine, A.L., Kramer, V.G., Siddappa, N.B., Xu, W., Else, J.G., Novembre, F.J., Strobert, E., O'Neil, S.P., Ruprecht, R.M., 2008. SHIV-1157i and passaged progeny viruses encoding R5 HIV-1 clade C env cause AIDS in rhesus monkeys. Retrovirology 17 (5), 94.

Igarashi, T., Endo, Y., Englund, G., Sadjadpour, R., Matano, T., Buckler, C., Buckler-White, A., Plishka, R., Theodore, T., Shibata, R., Martin, M., 1999. Emergence of a highly pathogenic simian/human immunodeficiency virus in a rhesus macaque treated with anti-CD8 mAb during a primary infection with a nonpathogenic virus. Proc. Natl. Acad. Sci. U. S. A. 96 (24), 14049–14054.

Igarashi, T., Donau, O.K., Imamichi, H., Dumaurier, M.J., Sadjadpour, R., Plishka, R.J., Buckler-White, A., Buckler, C., Suffredini, A.F., Lane, H.C., Moore, J.P., Martin, M.A., 2003. Macrophage-tropic simian/human immunodeficiency virus chimeras use CXCR4, not CCR5, for infections of rhesus macaque peripheral blood mononuclear cells and alveolar macrophages. J. Virol. 77 (24), 13042–13052.

Kozyrev, I.L., Miura, T., Takemura, T., Kuwata, T., Ui, M., Ibuki, K., Iida, T., Hayami, M., 2002. Co-expression of interleukin-5 influences replication of simian/human immunodeficiency viruses in vivo. J. Gen. Virol. 83, 1183–1188.

Jensen, M.A., Li, F.S., van 't Wout, A.B., Nickle, D.C., Shriner, D., He, H.X., McLaughlin, S., Shankarappa, R., Margolick, J.B., Mullins, J.I., 2003. Improved coreceptor usage prediction and genotypic monitoring of R5-to-X4 transition by motif analysis of human immunodeficiency virus type 1 env V3 loop sequences. J. Virol. 77 (24), 13376–13388.

Kestler III, H.W., Ringler, D.J., Mori, K., Panicali, D.L., Sehgal, P.K., Daniel, M.D., Desrosiers, R.C., 1991. Importance of the nef gene for maintenance of high virus loads and for development of AIDS. Cell 65 (4), 651–662.

Laird, M.E., Igarashi, T., Martin, M.A., Desrosiers, R.C., 2008. Importance of the V1/V2 loop region of simian–human immunodeficiency virus envelope glycoprotein gp120 in determining the strain specificity of the neutralizing antibody response. J. Virol. 82 (22), 11054–11065.

Li, M., Gao, F., Mascola, J.R., Stamatatos, L., Polonis, V.R., Koutsoukos, M., Voss, G., Goepfert, P., Gilbert, P., Greene, K.M., Bilska, M., Kothe, D.L., Salazar-Gonzalez, J.F., Wei, X., Decker, J.M., Hahn, B.H., Montefiori, D.C., 2005. Human immunodeficiency virus type 1 env clones from acute and early subtype B infections for standardized assessments of vaccine-elicited neutralizing antibodies. J. Virol. 79 (16), 10108–10125.

Luciw, P.A., Pratt-Lowe, E., Shaw, K.E., Levy, J.A., Cheng-Mayer, C., 1995. Persistent infection of rhesus macaques with T-cell-line-tropic and macrophage-tropic clones of simian/human immunodeficiency viruses (SHIV). Proc. Natl. Acad. Sci. U. S. A. 92 (16), 7490–7494.

Marcon, L., Choe, H., Martin, K.A., Farzan, M., Ponath, P.D., Wu, L., Newman, W., Gerard, N., Gerard, C., Sodroski, J., 1997. Utilization of C-C chemokine receptor 5 by the envelope glycoproteins of a pathogenic simian immunodeficiency virus, SIV-mac239. J. Virol. 71 (3), 2522–2527.

Margolis, L., Shattock, R., 2006. Selective transmission of CCR5-utilizing HIV-1: the 'gatekeeper' problem resolved? Nat. Rev. Microbiol. 4 (4), 312–317.

Mascola, J.R., Stiegler, G., VanCott, T.C., Katinger, H., Carpenter, C.B., Hanson, C.E., Beary, H., Hayes, D., Frankel, S.S., Birx, D.L., Lewis, M.G., 2000. Protection of macaques against vaginal transmission of a pathogenic HIV-1/SIV chimeric virus by passive infusion of neutralizing antibodies. Nat. Med. 6 (2), 207–210.

Mefford, M.E., Gorry, P.R., Kunstman, K., Wolinsky, S.M., Gabuzda, D., 2008. Bioinformatic prediction programs underestimate the frequency of CXCR4 usage by R5X4 HIV type 1 in brain and other tissues. AIDS Res. Hum. Retroviruses 24 (9), 1215–1220.

Miyake, A., Ibuki, K., Enose, Y., Suzuki, H., Horiuchi, R., Motohara, M., Saito, N., Nakasone, T., Honda, M., Watanabe, T., Miura, T., Hayami, M., 2006. Rapid dissemination of a pathogenic simian/human immunodeficiency virus to systemic organs and active replication in lymphoid tissues following intrarectal infection. J. Gen. Virol. 87, 1311–1320.

Nishimura, Y., Igarashi, T., Donau, O.K., Buckler-White, A., Buckler, C., Lafont, B.A., Goeken, R.M., Goldstein, S., Hirsch, V.M., Martin, M.A., 2004. Highly pathogenic SHIVs and SIVs target different CD4+ T cell subsets in rhesus monkeys, explaining their divergent clinical courses. Proc. Natl. Acad. Sci. U. S. A. 101 (33), 12324–12329.

O'Doherty, U., Swiggard, W.J., Malim, M.H., 2000. Human immunodeficiency virus type 1 spinoculation enhances infection through virus binding. J. Virol. 74, 10074–10080.

Pastore, C., Ramos, A., Mosier, D.E., 2000. Intrinsic obstacles to human immunodeficiency virus type 1 coreceptor switching. J. Virol. 74 (15), 6769–6776.

Pitcher, C.J., Hagen, S.I., Walker, J.M., Lum, R., Mitchell, B.L., Maino, V.C., Axthelm, M.K., Picker, L.J., 2002. Development and homeostasis of T cell memory in rhesus macaque. J. Immunol. 168 (1), 29–43.

Reimann, K.A., Li, J.T., Veazey, R., Halloran, M., Park, I.W., Karlsson, G.B., Sodroski, J., Letvin, N.L., 1996. A chimeric simian/human immunodeficiency virus expressing a primary patient human immunodeficiency virus type 1 isolate env causes an AIDS-like disease after in vivo passage in rhesus monkeys. J. Virol. 70 (10), 6922–6928.

Sadjadpour, R., Theodore, T.S., Igarashi, T., Donau, O.K., Plishka, R.J., Buckler-White, A., Martin, M.A., 2004. Induction of disease by a molecularly cloned highly pathogenic simian immunodeficiency virus/human immunodeficiency virus chimera is multigenic. J. Virol. 78, 5513–5519.

Sagar, M., Wu, X., Lee, S., Overbaugh, J., 2006. Human immunodeficiency virus type 1 V1-V2 envelope loop sequences expand and add glycosylation sites over the course of infection, and these modifications affect antibody neutralization sensitivity. J. Virol. 80 (19), 9586–9598.

Shibata, R., Kawamura, M., Sakai, H., Hayami, M., Ishimoto, A., Adachi, A., 1991. Generation of a chimeric human and simian immunodeficiency virus infectious to monkey peripheral blood mononuclear cells. J. Virol. 65 (7), 3514–3520.

Shimizu, Y., Okoba, M., Yamazaki, N., Goto, Y., Miura, T., Hayami, M., Hoshino, H., Haga, T., 2006. Construction and in vitro characterization of a chimeric simian and human immunodeficiency virus with the RANTES gene. Microbes. Infect. 8 (1), 105–113.

Shinohara, K., Sakai, K., Ando, S., Ami, Y., Yoshino, N., Takahashi, E., Someya, K., Suzaki, Y., Nakasone, T., Sasaki, Y., Kaizu, M., Lu, Y., Honda, M., 1999. A highly pathogenic simian/human immunodeficiency virus with genetic changes in cynomolgus monkey. J. Gen. Virol. 80, 1231–1240.

Shiver, J.W., Fu, T.M., Chen, L., Casimiro, D.R., Davies, M.E., Evans, R.K., Zhang, Z.Q., Simon, A.J., Trigona, W.L., Dubey, S.A., Huang, L., Harris, V.A., Long, R.S., Liang, X., Handt, L., Schleif, W.A., Zhu, L., Freed, D.C., Persaud, N.V., Guan, L., Punt, K.S., Tang, A., Chen, M., Wilson, K.A., Collins, K.B., Heidecker, G.J., Fernandez, V.R., Perry, H.C., Joyce, J.G., Grimm, K.M., Cook, J.C., Keller, P.M., Kresock, D.S., Mach, H., Troutman, R.D., Isopi, L.A., Williams, D.M., Xu, Z., Bohannon, K.E., Volkin, D.B., Montefiori, D.C., Miura, A., Krivulka, G.R., Lifton, M.A., Kuroda, M.J., Schmitz, J.E., Letvin, N.L., Caulfield, M.J., Bett, A.J., Youil, R., Kaslow, D.C., Emini, E.A., 2002. Replication-incompetent adenoviral vaccine vector elicits effective anti-immunodeficiency-virus immunity. Nature 415 (6869), 331–335.

Sing, T., Low, A.J., Beerenwinkel, N., Sander, O., Cheung, P.K., Domingues, F.S., Büch, J., Däumer, M., Kaiser, R., Lengauer, T., Harrigan, P.R., 2007. Predicting HIV coreceptor usage on the basis of genetic and clinical covariates. Antivir. Ther. 12 (7), 1097–1106.

Tan, R.C., Harouse, J.M., Gettie, A., Cheng-Mayer, C., 1999. In vivo adaptation of SHIV (SF162): chimeric virus expressing a NSI, CCR5-specific envelope protein. J. Med. Primatol. 28 (4-5), 164–168.

Trkola, A., Kuhmann, S.E., Strizki, J.M., Maxwell, E., Ketas, T., Morgan, T., Pugach, P., Xu, S., Wojcik, L., Tagat, J., Palani, A., Shapiro, S., Clader, J.W., McCombie, S., Reyes, G.R., Baroudy, B.M., Moore, J.P., 2002. HIV-1 escape from a small molecule, CCR5-specific entry inhibitor does not involve CXCR4 use. Proc. Natl. Acad. Sci. U.S.A. 99, 395–400.

Veazey, R.S., DeMaria, M., Chalifoux, L.V., Shvetz, D.E., Pauley, D.R., Knight, H.L., Rosenzweig, M., Johnson, R.P., Desrosiers, R.C., Lackner, A.A., 1998. Gastrointestinal tract as a major site of CD4+ T cell depletion and viral replication in SIV infection. Science 280 (5362), 427–431.

Wei, X., Decker, J.M., Wang, S., Hui, H., Kappes, J.C., Wu, X., Salazar-Gonzalez, J.F., Salazar, M.G., Kilby, J.M., Saag, M.S., Komarova, N.L., Nowak, M.A., Hahn, B.H., Kwong, P.D., Shaw, G.M., 2003. Antibody neutralization and escape by HIV-1. Nature 422 (6929), 307–312.

Willey, R.L., Smith, D.H., Lasky, L.A., Theodore, T.S., Earl, P.L., Moss, B., Capon, D.J., Martin, M.A., 1988. In vitro mutagenesis identifies a region within the envelope gene of the human immunodeficiency virus that is critical for infectivity. J. Virol. 62 (1), 139–147.

Yamaguchi-Kabata, Y., Yamashita, M., Ohkura, S., Hayami, M., Miura, T., 2004. Linkage of amino acid variation and evolution of human immunodeficiency virus type 1 gp120 envelope glycoprotein (subtype B) with usage of the second receptor. J. Mol. Evol. 58 (3), 333–340.

Zhang, Y., Lou, B., Lal, R.B., Gettie, A., Marx, P.A., Moore, J.P., 2000. Use of inhibitors to evaluate coreceptor usage by simian and simian/human immunodeficiency viruses and human immunodeficiency virus type 2 in primary cells. J. Virol. 74 (15), 6893–6910.

Web references

Web PSSM, Mullins Lab, University of Washington http://indra.mullins.microbiol.washington.edu/webpssm/

Geno2pheno [coreceptor], Max-Planck-Institut Informatik. http://coreceptor.bioinf.mpi-inf.mpg.de

Journal of General Virology (2010), **91**, 773–781 DOI 10.1099/vir.0.017368-0

Small intestine CD4$^+$ cell reduction and enteropathy in simian/human immunodeficiency virus KS661-infected rhesus macaques in the presence of low viral load

Katsuhisa Inaba,[1] Yoshinori Fukazawa,[1] Kenta Matsuda,[1] Ai Himeno,[1] Megumi Matsuyama,[1] Kentaro Ibuki,[1] Yoshiharu Miura,[2] Yoshio Koyanagi,[2] Atsushi Nakajima,[3] Richard S. Blumberg,[4] Hidemi Takahashi,[5] Masanori Hayami,[1] Tatsuhiko Igarashi[1] and Tomoyuki Miura[1]

Correspondence
Tomoyuki Miura
tmiura@virus.kyoto-u.ac.jp

[1]Laboratory of Primate Model, Experimental Research Center for Infectious Diseases, Institute for Virus Research, Kyoto University, 53 Shogoinkawaramachi, Sakyo-ku, Kyoto 606-8507, Japan

[2]Laboratory of Viral Pathogenesis, Institute for Virus Research, Kyoto University, 53 Shogoinkawaramachi, Sakyo-ku, Kyoto 606-8507, Japan

[3]Division of Gastroenterology, Yokohama City University Graduate School of Medicine, Yokohama, Japan

[4]Division of Gastroenterology, Brigham and Women's Hospital, Harvard Medical School, Boston, MA, USA

[5]Department of Microbiology and Immunology, Nippon Medical School, Tokyo, Japan

Received 5 October 2009
Accepted 3 November 2009

Human immunodeficiency virus type 1, simian immunodeficiency virus and simian/human immunodeficiency virus (SHIV) infection generally lead to death of the host accompanied by high viraemia and profound CD4$^+$ T-cell depletion. SHIV clone KS661-infected rhesus macaques with a high viral load set point (HVL) ultimately experience diarrhoea and wasting at 6–12 months after infection. In contrast, infected macaques with a low viral load set point (LVL) usually live asymptomatically throughout the observation period, and are therefore referred to as asymptomatic LVL (Asym LVL) macaques. Interestingly, some LVL macaques exhibit diarrhoea and wasting similar to the symptoms of HVL macaques and are termed symptomatic LVL (Sym LVL) macaques. This study tested the hypothesis that Sym LVL macaques have the same degree of intestinal abnormalities as HVL macaques. The proviral DNA loads in lymphoid tissue and the intestines of Sym LVL and Asym LVL macaques were comparable and all infected monkeys showed villous atrophy. Notably, the CD4$^+$ cell frequencies of lymphoid tissues and intestines in Sym LVL macaques were remarkably lower than those in Asym LVL and uninfected macaques. Furthermore, Sym LVL and HVL macaques exhibited an increased number of activated macrophages. In conclusion, intestinal disorders including CD4$^+$ cell reduction and abnormal immune activation can be observed in SHIV-KS661-infected macaques independent of virus replication levels.

INTRODUCTION

The intestinal tract, which is the largest mucosal and lymphoid organ and which contains the majority of the total lymphocytes in the body, is an important port of entry for human immunodeficiency virus type 1 (HIV-1) infection in vertical and homosexual transmission (Smith *et al.*, 2003). Additionally, the intestinal tract is a central site in the interaction between HIV-1 and its host, and suffers profound pathological changes as a result of HIV-1 infection. HIV-1 infection of the intestinal tract is characterized by virus replication (Fackler *et al.*, 1998), CD4$^+$ T-cell depletion (Brenchley *et al.*, 2004), opportunistic infection and HIV enteropathy, which is an idiopathic intestinal disorder observed in infected patients with diarrhoea (Kotler, 2005). In particular, CD4$^+$ T-cell depletion, which is the immunological hallmark in the development of AIDS, preferentially takes place in the intestinal tract rather than in the peripheral blood throughout the infection (Brenchley *et al.*, 2004). This

observation is based on the following findings: (i) most naturally transmitted HIV-1 strains are chemokine receptor 5 (CCR5)-tropic; and (ii) the intestinal tract, especially the lamina propria, contains a large number of activated memory $CCR5^+$ $CD4^+$ T cells, which indicates a high susceptibility for HIV-1 infection, whereas the peripheral blood has a relatively small population of these cells (Anton *et al.*, 2000; Lapenta *et al.*, 1999). $CD4^+$ T-cell depletion from the intestinal tract by HIV-1 infection is thought to lead to progressive dysfunction of mucosal immunity, which triggers immunodeficiency (Paiardini *et al.*, 2008). In addition to $CD4^+$ T-cell depletion in the intestinal tract, HIV-1 infection causes histopathological changes in the intestine, including villous atrophy, crypt hyperplasia and acute/chronic inflammation (Batman *et al.*, 1989).

Chronic disease of the intestinal tract generally manifests as inflammation (Kahn, 1997). Diarrhoea is a major intestinal symptom caused by various stimuli to the intestinal tract such as pathogens, toxins and dysfunction of the immune system (Gibbons & Fuchs, 2007). Because HIV-1 infection weakens the host immune system, AIDS is one of the primary causes of chronic diarrhoea (Sestak, 2005). In developing countries, diarrhoea was a major symptom in advanced HIV-1 infection prior to the establishment of highly active antiretroviral therapy (HAART) (Wilcox & Saag, 2008). Dehydration and malabsorption as a result of chronic diarrhoea can lead to progressive weight loss and can contribute to morbidity and mortality in HIV-1-infected patients (Sharpstone & Gazzard, 1996). Therefore, chronic diarrhoea is one of the most important clinical signs in AIDS patients.

AIDS models using non-human primates have provided many important observations on AIDS pathogenesis. The first finding of early $CD4^+$ T-cell depletion from the intestinal tract was reported in a study using simian immunodeficiency virus (SIV)-infected macaques (Veazey *et al.*, 1998). Intestinal $CD4^+$ T cells of rhesus macaques predominantly exhibit a $CCR5^+$ activated memory phenotype, and $CD4^+$ T cells of this phenotype are selectively eliminated in SIV-infected macaques, indicating that the majority of intestinal $CD4^+$ T cells are primary targets of SIV infection (Veazey *et al.*, 2000a, b). Accordingly, detailed analysis of the intestinal tract using animal models is essential for an understanding of AIDS pathogenesis.

Simian/human immunodeficiency virus (SHIV)-KS661 is a molecular clone and a pathogenic virus in rhesus macaques. SHIV-KS661 systemically depletes $CD4^+$ T cells of rhesus macaques within 4 weeks of infection (Miyake *et al.*, 2006). Based on our observations over a number of years, intravenous infection of rhesus macaques with SHIV-KS661 consistently results in high viraemia and $CD4^+$ T-cell depletion, followed by malignant morbidity as a result of severe chronic diarrhoea and wasting after 6–18 months. Generally, the time to clinical morbidity in rhesus macaques infected with pathogenic SHIVs, such as SHIV-89.6P and SHIV-KS661, is considerably shorter than in HIV-1-infected humans, who take an average of 10 years to progress to AIDS. In addition, all subsets of $CD4^+$ T cells including memory and naïve T cells are thoroughly depleted in pathogenic SHIV-infected macaques. However, in the SHIV-KS661 macaque model, diarrhoea and wasting, which are major symptoms in advanced HIV-1 infection, can clearly be recognized and defined in association with disease progression.

Recently, we observed that, in many rhesus macaques infected intrarectally with SHIV-KS661, plasma viral RNA loads decreased gradually to undetectable levels in the chronic phase, which is quite different from the case with intravenous infection. It is well known that pathogenic SIV and SHIV infections in monkeys, like HIV-1 infections in humans, generally lead to high viraemia, profound $CD4^+$ T-cell depletion and death. Interestingly, in this study, two out of six intrarectally inoculated macaques with a low plasma viral load experienced malignant morbidity manifest as severe diarrhoea and wasting, similar to what we observed in infected macaques with high viraemia. The purpose of this study was to elucidate why macaques with a low plasma viral load experienced diarrhoea and wasting. As an explanation for this morbidity, we hypothesized that, even if the viral load set-point is suppressed, SHIV-KS661-infected macaques would have the same degree of intestinal abnormalities as infected macaques with high viraemia. To test this hypothesis, we analysed $CD4^+$ cell frequencies in lymphoid and intestinal tissues and damage to the intestinal mucosa in infected macaques with high and low viral load set points (HVL and LVL, respectively). Here, we have provided evidence for the development of intestinal disorders in SHIV-KS661-infected macaques irrespective of the plasma viral RNA load.

RESULTS

Diarrhoea and wasting in two macaques despite low viral load

All macaques inoculated intravenously with SHIV-KS661 and one out of seven macaques inoculated intrarectally with SHIV-KS661 exhibited high set points of plasma viral RNA loads, persisting at over 10^6 copies ml^{-1} until they needed to be euthanized as a result of diarrhoea and wasting (Fig. 1a). In contrast, in the remaining six macaques inoculated intrarectally with SHIV-KS661, the set points of plasma viral RNA load gradually decreased to undetectable levels (Fig. 1a). We called these macaques showing high and low set points of viral RNA load HVL and LVL macaques, respectively. During an observation period of approximately 1.4 years, two LVL macaques (MM397 and MM399) experienced severe diarrhoea and wasting and required euthanasia at approximately 22 weeks post-infection (p.i.), similar to HVL macaques, whereas the remaining four LVL macaques were asymptomatic (Fig. 1a). We termed the healthy LVL macaques asymptomatic LVL macaques (Asym LVL) and the LVL

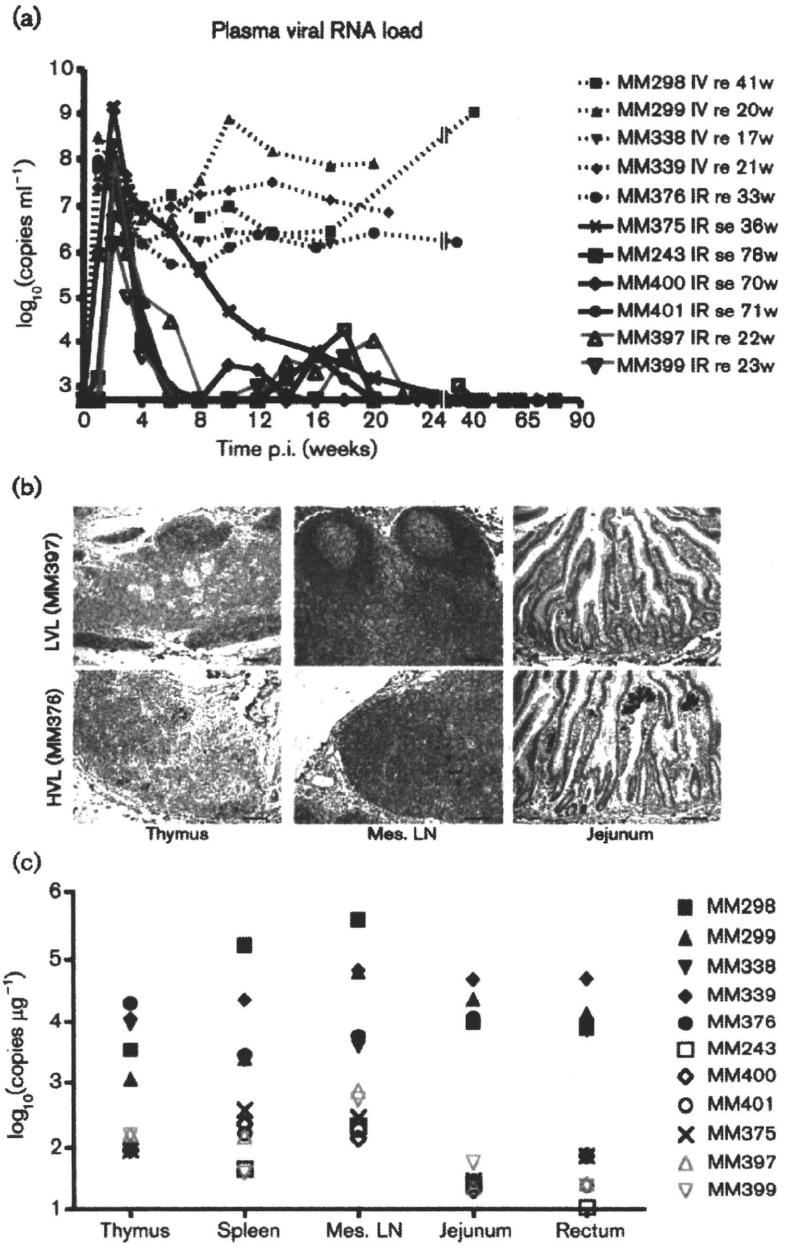

Fig. 1. Distribution of virus in various tissues of SHIV-KS661-infected rhesus macaques. (a) Time course of plasma viral RNA loads as measured by quantitative RT-PCR. The detection limit of plasma viral RNA loads was 500 copies ml^{-1}. The animal ID numbers, infection route and when and how they were euthanized are indicated on the figure. IV, Intravenous inoculation; IR, intrarectal inoculation; re, required euthanasia; se, scheduled euthanasia; w, number of weeks after infection when euthanasia was performed. (b) Immunohistochemical detection of Nef antigen in thymus, mesenteric lymph nodes (Mes. LN) and jejunum. Brown staining indicates Nef^+ cells. The upper panels show representative tissue sections from a Sym LVL macaque (MM397) and the lower panels show representative tissue sections from an HVL macaque (MM376). Bars, 100 µm. (c) Proviral DNA loads in different tissues of SHIV-KS661-infected macaques, as measured by quantitative PCR. The detection limit of proviral DNA loads was 10 copies μg^{-1}. Filled black symbols indicate HVL macaques, open black symbols indicate Asym LVL macaques and open grey symbols indicate Sym LVL macaques.

macaques with diarrhoea and wasting symptomatic LVL macaques (Sym LVL).

Antibody response against SHIV in infected macaques

The LVL macaques showed antibody responses to SHIV-KS661 at 3–4 weeks p.i. and then developed strong antibody responses that persisted up to 18 weeks p.i. (Table 1). In contrast, two of the HVL macaques (MM298 and MM299) showed no antibody response, whilst the remaining two (MM338 and MM339) showed very low antibody responses. Among the HVL macaques, only MM376 showed a strong antibody response: the titre reached 1:2048 at 6 weeks p.i., but then decreased to a much lower value. These results showed that LVL macaques succeeded in maintaining a strong antibody response, whilst HVL macaques failed to do so.

Viral levels in tissues from Sym LVL and Asym LVL macaques are not significantly different

To investigate whether the infected macaques had different viral levels in their lymphoid and intestinal tissues, we used

Table 1. Anti-HIV antibody titres in infected monkeys

– indicates a titre of <32.

Time (weeks)	Intrarectal inoculation						Intravenous inoculation				
	LVL						HVL				
	MM243	MM397	MM399	MM400	MM401	MM375	MM376	MM298	MM299	MM338	MM339
0	–	–	–	–	–	–	–	–	–	–	–
1	–	–	–	–	–	–	–	–	–	–	–
2	–	–	–	–	–	–	–	–	–	64	64
3	32	–	32	–	–	128	–	–	–	32	32
4	32	16384	32	64	32	512	512	–	–	–	–
6	8192	16384	256	64	4096	1024	2048	–	–	–	–
8	4096	16384	1024	128	1024	16384	512	–	–	–	–
10	16384	16384	2048	512	512	16384	512	–	–	–	–
12	16384	16384	256	512	4096	16384	512				
13								–	–	–	–
14	16384	16384	1024	512	2048						
16	4096	8192	1024	1024	1024	16384	64				
17								–	–	–	–
18	8192	16384	2048	8192	4096						

the Nef antigen as a marker of virus infection using immunohistochemistry and quantitative analysis of proviral DNA in lymphoid and intestinal tissues. Nef^+ cells were detected in large numbers in the tissues of HVL macaques, but were undetectable in both Sym LVL (Fig. 1b) and Asym LVL (data not shown) macaques.

In the HVL macaques, high proviral DNA loads (>1000 copies μg^{-1}) were found in all of the tissues examined (Fig. 1c). In contrast, the proviral DNA loads in the tissues of the LVL macaques were only several tens to several hundreds of copies μg^{-1} (Fig. 1c). Furthermore, Sym LVL and Asym LVL macaques exhibited comparably low proviral DNA loads in these tissues (Fig. 1c). The low viral levels in lymphoid and intestinal tissues in the LVL macaques were consistent with their set points of plasma viral RNA loads. The viral levels in lymphoid and intestinal tissues were not significantly different between Sym LVL and Asym LVL macaques.

Diarrhoea and wasting in LVL macaques correlate with $CD4^+$ cell frequency in lymphoid and intestinal tissues, but not in peripheral blood

Because $CD4^+$ T-cell depletion is the hallmark of AIDS, we first examined $CD4^+$ T-cell counts in peripheral blood. Whilst peripheral $CD4^+$ T cells were completely and irreversibly depleted in HVL macaques throughout the infection, they displayed various kinetics in LVL macaques (Fig. 2a). MM397 (Sym LVL) and MM401 (Asym LVL) had very low $CD4^+$ T-cell counts (<150 cells ml^{-1}) at all times at which they were examined after infection, whereas MM399 (Sym LVL) and MM400 (Asym LVL) maintained moderate $CD4^+$ T-cell counts (>300 cells ml^{-1}) throughout the experiment (Fig. 2a).

Naïve $CD4^+$ T cells of MM397 (Sym LVL), MM243 (Asm LVL) and MM401 (Asym LVL) were depleted as early as 4 weeks p.i., whereas those of MM399 (Sym LVL) and MM400 (Asym LVL) remained at moderate levels (Fig. 2b). The HVL macaques were not examined because their peripheral $CD4^+$ T cells were depleted.

In addition to evaluating $CD4^+$ T cells in the blood, we evaluated $CD4^+$ cells in lymphoid and intestinal tissues using CD4 staining. The HVL macaques showed severe depletion of $CD4^+$ cells in all lymphoid tissues and intestine compared with the uninfected macaques (Fig. 2c, d). Interestingly, the $CD4^+$ cell frequencies in the tissues were clearly lower in Sym LVL macaques than in uninfected macaques (Fig. 2c, d). However, the $CD4^+$ cell frequencies in the tissues of Asym LVL macaques were comparable to those in uninfected macaques. These findings indicated that the emergence of diarrhoea and wasting in LVL macaques correlated with the low $CD4^+$ cell frequency in lymphoid tissues and the intestines, but not with the counts of peripheral $CD4^+$ T-cell subsets.

Infected animals exhibit significantly shorter villi

Symptomatic animals (Sym LVL and HVL macaques) exhibited diarrhoea. To examine whether the jejunum of symptomatic animals exhibited the histopathological changes that suggest AIDS-related enteropathy, we measured villous length on haematoxylin and eosin (H&E)-stained samples of jejunum in uninfected and infected macaques. Surprisingly, villous length was significantly

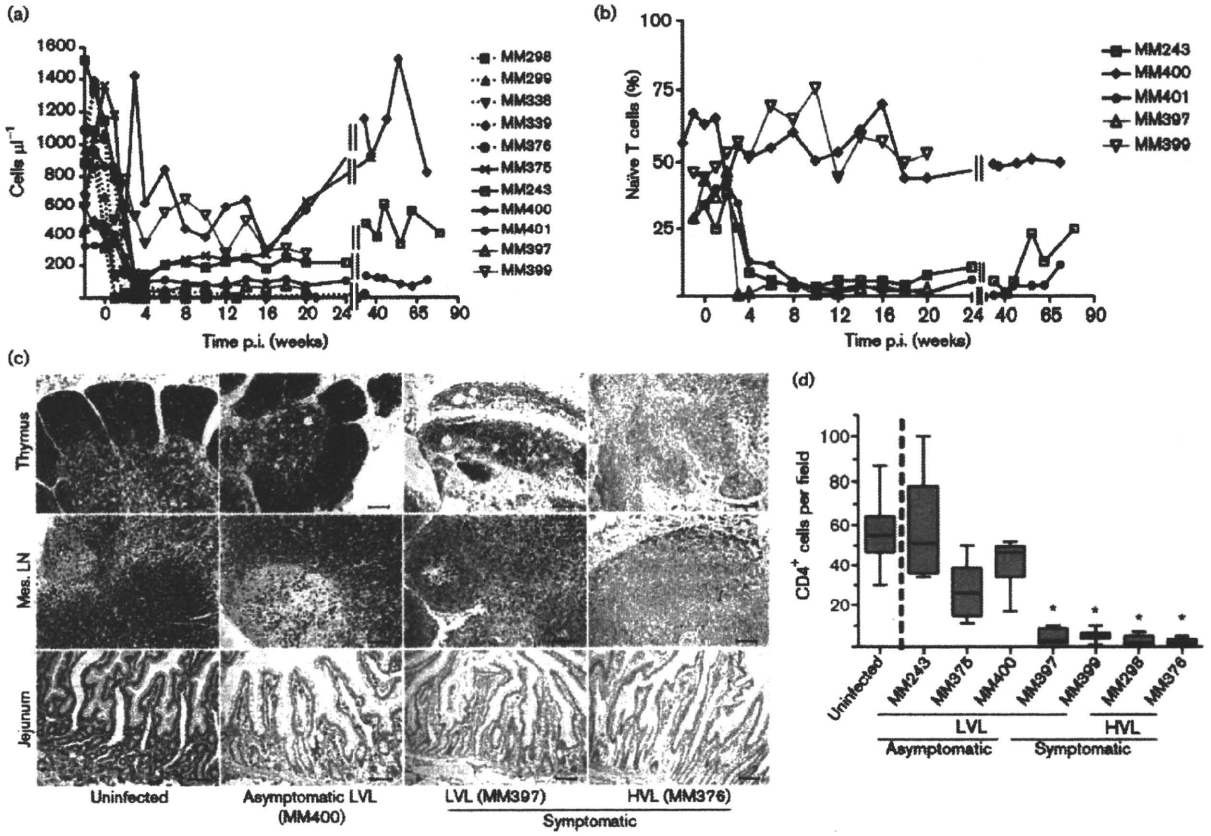

Fig. 2. Counts of circulating $CD4^+$ T-cell subsets and $CD4^+$ cell frequency in lymphoid and intestinal tissues at the time of euthanasia in SHIV-KS661-infected rhesus macaques. Counts of circulating $CD4^+$ T-cell subsets were analysed by flow cytometry and whole-blood counts. (a) Circulating $CD4^+$ T-cell counts. The ID numbers of the macaques are indicated on the figure. (b) Proportion of $CD95^+$ naïve cells in circulating $CD4^+$ T cells of LVL macaques. Solid black lines indicate Asym LVL macaques and solid grey lines indicate Sym LVL macaques. (c) $CD4^+$ cell frequencies in thymus, mesenteric lymph nodes (Mes. LN) and jejunum of representative uninfected, Asym LVL, Sym LVL and HVL macaques. Bars, 100 µm. (d) Quantification of jejunum $CD4^+$ cells in uninfected and infected macaques. The numbers of $CD4^+$ cells were enumerated in at least ten fields of the tissues at a magnification of 200×. Statistical analysis was performed using Student's *t*-test for the data from five uninfected and each infected macaque (*, $P<0.0001$). Data for MM299, MM338, MM339 and MM401 were not available.

shorter in all of the infected animals than in uninfected animals ($P<0.0001$) (Fig. 3a, b). This suggested that SHIV-infected animals develop villous atrophy, irrespective of viral load.

Increased number of activated macrophages in the jejunum of symptomatic animals

Macrophages appeared to be more abundant in H&E-stained jejunal sections in symptomatic animals. This was confirmed by CD68 staining: the frequency of $CD68^+$ macrophages in the jejunum was considerably higher in symptomatic animals than in uninfected animals, but was not significantly different between uninfected animals and Asym LVL macaques (data not shown). Furthermore, $CD68^+$ macrophages in the small intestine of Sym LVL and HVL macaques appeared to be activated because their size was increased. To examine whether the number of activated $CD68^+$ macrophages increased in the small intestine, we double stained for CD68 and Ki67 in the small intestine sections by immunohistochemistry. The frequency of $CD68^+$ $Ki67^+$ macrophages in the jejunum of all symptomatic animals examined was significantly higher than that of uninfected animals ($P<0.0001$) (Fig. 3c, d). This suggested that abnormal activation of intestinal macrophages occurred in symptomatic animals irrespective of viral load.

DISCUSSION

It is important to discuss initially why some SHIV-infected macaques had an HVL at the late stage, whilst others had